



저작자표시-비영리-변경금지 2.0 대한민국

이용자는 아래의 조건을 따르는 경우에 한하여 자유롭게

- 이 저작물을 복제, 배포, 전송, 전시, 공연 및 방송할 수 있습니다.

다음과 같은 조건을 따라야 합니다:



저작자표시, 귀하는 원저작자를 표시하여야 합니다.



비영리, 귀하는 이 저작물을 영리 목적으로 이용할 수 없습니다.



변경금지, 귀하는 이 저작물을 개작, 변형 또는 가공할 수 없습니다.

- 귀하는, 이 저작물의 재이용이나 배포의 경우, 이 저작물에 적용된 이용허락조건을 명확하게 나타내어야 합니다.
- 저작권자로부터 별도의 허가를 받으면 이러한 조건들은 적용되지 않습니다.

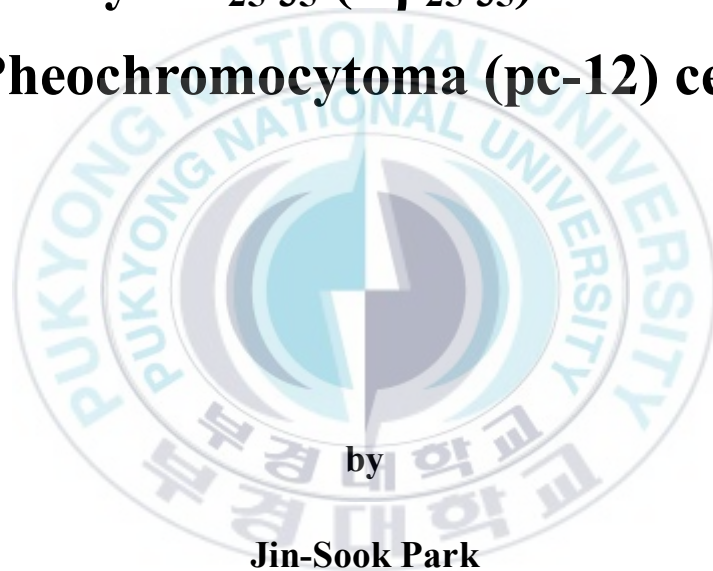
저작권법에 따른 이용자의 권리는 위의 내용에 의하여 영향을 받지 않습니다.

이것은 [이용허락규약\(Legal Code\)](#)을 이해하기 쉽게 요약한 것입니다.

[Disclaimer](#)

Thesis for the Degree of Master of Science

**Inhibitory Effect of Chitooligosaccharide on
Neuronal Apoptosis Induced by Beta
amyloid₂₅₋₃₅ ($A\beta_{25-35}$) in Rat
Pheochromocytoma (pc-12) cell**



by

Jin-Sook Park

Department of Chemistry

The Graduate School

Pukyong National University

February 2008

Inhibitory Effect of Chitooligosaccharide on Neuronal Apoptosis Induced by Beta-amyloid₂₅₋₃₅ (A β ₂₅₋₃₅) in Rat Pheochromocytoma (pc-12) cell

쥐의 갈색세포종을 이용한 키토산 올리고당의 Beta-amyloid₂₅₋₃₅ (A β ₂₅₋₃₅)에 의해 유발되는

세포자멸사 저해 효과

Advisor : Prof. Se-Kwon Kim

by

Jin-Sook Park

A thesis submitted in partial fulfillment of the requirements

for the degree of

Master of Science

in the Department of Chemistry, Graduate School

Pukyong National University

February 2008

**Inhibitory Effect of Chitooligosaccharide on Neuronal Apoptosis
Induced by Beta-amyloid₂₅₋₃₅ (A β ₂₅₋₃₅) in Rat Pheochromocytoma
(pc-12) cell**

A dissertation

by

Jin-Sook Park


Approved as to style and content by:



Prof. Hyun-Kwan Shim (Chairman)



Prof. So-Won Youn (Member)



Prof. Se-Kwon Kim (Member)

February, 2008

Inhibitory Effect of Chitooligosaccharide on Neuronal Apoptosis Induced by Beta-amyloid $A\beta_{25-35}$ in Rat Pheochromocytoma (pc-12) cells

Jin-Sook Park

**Department of Chemistry, Graduate School,
Pukyung National University**

Abstract

Alzheimer disease (AD) is the most common age-related neurodegenerative disorder that affects the brain, and the cause of dementia in the elderly. The major factor of AD is the beta-amyloid ($A\beta$), which generates reactive oxygen species (ROS) in the cell. In this research, we evaluated the inhibition of COS on the ROS-induced apoptosis generated by $A\beta_{25-35}$ in the rat pheochromocytoma (pc-12) cells. Treatment of COS showed the increasing inhibitory effect on gene and protein expression levels of not only p53 and p21 but also other apoptosis-related genes such as caspases, cytochrom c, and Apaf-1. Cell cycle analysis of pc-12 cells in the presence of COS confirmed that COS reduced cell cycle arrest at S phase. These result showed that COS is effective to inhibit the formation ROS, therefore, COS can inhibit neuronal apoptosis induced by $A\beta_{25-35}$ in the pc-12 cells. Moreover, there are some evidences that acetylcholinesterase (AChE) plays a key role in modulating the cytotoxicity of $A\beta$. This research also showed that COS can inhibit AChE activity. These results suggest that COS has potential ability as a restrainer of AD.

Table of Contents

Abstract	i
Table of Content	ii
List of Figures	iv
List of Tables	vi
Abbreviation	vii
Introduction	1
Experimental Procedures	
1. Materials	18
2. Preparation of chitosan oligosaccharides using an UF membrane bioreactor.....	18
3. Sample preparation.....	20
4. Cell culture	20
5. Cell Viability (MTT Assay).....	21
6. Acetyl cholinesterase (AChE) inhibitory activity	21
7. Cellular ROS determination by DCFH-DA	23
8. Fluorescence microscopy analysis.....	23
9. Terminal deoxynucleotidyl transferase biotin-dUTP nick end labeling (TUNEL) assay	23
10. Cell cycle analysis by flow cytometry	24
11. RNA extraction.....	25
12. Real-time polymerase chain reaction (Real-time PCR).....	25
13. Western Blot assay.....	28
14. Measurement of total protein concentration.....	28
15. Statistical analysis	28

Result and discussion

1. pH of COS and culture media	29
2. Effect of COS on viability of pc-12 cells	29
3. COS inhibited AChE activity induced by A β ₂₅₋₃₅	32
4. Effect of COS on viability of pc-12 cells affected by A β ₂₅₋₃₅	35
5. Effect of COS on intracellular ROS level induced by A β ₂₅₋₃₅ in pc-12 cells	35
6. Morphological analysis of pc-12 cells affected by A β ₂₅₋₃₅ -induced apoptosis	38
7. Confirm of apoptotic cell death by TUNEL assay	38
8. Determination of apoptosis by cell cycle	41
9. COS inhibit apoptosis via reduction of p53 expression level	44
10. COS inhibited target genes in apoptosis pathway that affected by A β ₂₅₋₃₅	47
Summary	58
References	60

List of Figures

Figure 1. Cross-section of the brain.....	3
Figure 2. The amyloid- β ($A\beta$) peptide is derived via proteolysis from a larger precursor molecule called the amyloid precursor protein (APP).....	4.
Figure 3. Putative Amyloid Cascade.....	5
Figure 4. Activation and inhibition of apoptosis.	9
Figure 5. p53 signaling pathway.....	10
Figure 6. Caspase Cascade.	11
Figure 7. Oxidative damage due to the endogenous production of reactive oxygen species by mitochondria can lead to cell death via apoptosis.	12
Figure 8. Structure of Chiosan and Chitooligosaccharide (COS).	15
Figure 9. Schematic diagram of the dual reactor system developed for continuous production of chitooligosaccharide (COS).	20
Figure 10. Ellman 's assay for determination of AChE activity.	22
Figure 11. Cell viability of COS on pc-12 cell.	31
Figure 12. AChE activity	33
Figure 13. Western blot assay of AChE protein expression.....	34
Figure 14. Cell viability of COS and $A\beta_{25-35}$ on pc-12 cell	36
Figure 15. Cellular radical scavenging activity of COS	37
Figure 16. Morphological analysis of pc-12 treated with 1000 μ g COS and $A\beta$ (25 μ M).	39
Figure 17. TUNEL assay.....	40.
Figure 18. Cells cycle analysis of pc-12 cells in the presence of COS.....	42
Figure 19. Quantification of apoptosis in pc-12 cells treated with COS after PI staining	43

Figure 20. p53 mRNA expression in COS treated pc-12 cells.	45
Figure 21. Western blot assay of MDM2 and p21 protein expression in pc-12 cells treated with COS.....	46
Figure 22. Western blot assay of MDM2 and p21 protein expression in pc-12 cells treated with COS.....	49
Figure 23. Bcl-2 mRNA expression level treated pc-12 cells.....	50
Figure 24. Bax mRNA expression level in COS treated pc-12 cells.....	51
Figure 25. Western blot assay of Bax and Bcl-2 protein expression in pc-12 cells treated with COS.	52
Figure 26. Western blot assay of Apaf-1 and cytochrome C protein expression in pc-12 cells treated with COS.	53
Figure 27. Caspase-9 mRNA expression level in COS treated pc-12 cells.	55
Figure 28. Caspase-3 mRNA expression in COS treated pc-12 cells.	56
Figure 29. Western blot assay of caspase-9, caspase-3 and caspase-8 protein expression in pc- 12 cells treated with COS.....	57
Figure 30. The proposed signaling cascade in pc-12 cells affected by COS.....	59

List of Tables

Table 1. The sequences of the primer for real-time PCR	27
Table 2. pH of sample solution	30



List of Abbreviation

AD	Alzheimer disease
A β	beta-amyloid
APP	amyloid precursor protein
ROS	reactive oxygen species
PTP	permeability transition pore
AChE	acetylcholinesterase
COS	Chitooligosaccharides
pc-12	rat pheochromocytoma
EDTA	ethylene diamine tetraacetic acid
FBS	fetal bovine serum
MTT	3-(4,5-dimethyl-2-yl)-2,5-diphenyltetrazolium bromide
ATCh	Acetylthiocholine
DTNB	5,5'-dithiobis-(2-nitrobenzoic acid)
DCFH-DA	2',7'-Dichlorofluorecin diacetate
Apaf	apoptosis activating factor
DMSO	dimethyl sulfoxide
FACS	fluorescence activated cells
G3PDH	glyceraldehydes-3-phosphate dehydrogenase
PCR	phorbol myristate acetate
TUNEL	dUTP nick end labeling

Introduction

Alzheimer disease (AD), named for German physician Alois Alzheimer who first described it in 1906, is the most common age-related neurodegenerative disorder that affects the brain, and cause of dementia in the elderly. The incidence of AD is increasing at an alarming rate along with aging of populations of industrialized countries. The prevalence of AD among 60-year-olds is about 1%. This incidence doubles approximately every 5 years, becoming 2% at the age of 65 years, 8% at 75 years, and 16 and 32% at 85 years (Giorgio et al. 2006). The clinical symptoms result from the deterioration of selective domains, those related to memory. Memory decline initially manifests as a loss of episodic memory, which is considered a subcategory of declarative memory. The dysfunction in episodic memory impedes recollection of recent events including autobiographical activities (Frank et al. 2007). The memory loss results in behavioral deficit, disorientation in time and space, and impairments in language skills. These cognitive deficits have been linked to the loss of neurons in brain regions such as the cortex and hippocampus (Yan et al. 1996) (Fig. 1). There are three clinical stages of AD – mild, moderate and severe – with cognitive and functional decline stretching over 5–8 years. The initial stage usually lasts 2–3 years and is characterized by short-term memory impairment often accompanied by symptoms of anxiety and depression. In the moderate stage, these symptoms appear to abate as neuropsychiatric manifestations, such as visual hallucinations, false beliefs and reversal of sleep patterns emerge. The severe and final stage is characterized by motor signs, such as motor rigidity and prominent cognitive decline. Cognitive and functional decline tends to be linear throughout the three stages of the disease, whereas caregiver burden peaks with the onset of neuropsychiatric symptoms and declines somewhat during the final stage, when the

patient is more sedentary (Gauthier et al. 2002).

As stated above, the disease was named after the German psychologist Alois Alzheimer, but while he is the disease's namesake, his colleague Emil Kraepelin played a just as important role in the identification of the disease. Kraepelin isolated and grouped together the symptoms of the disorder, suggesting they were unique disease processes, while Alzheimer was the first to understand what was actually happening in the brains of Alzheimer's patients. In the early 1900's Alzheimer was following the case of a 51-year-old woman who exhibited the symptoms of the disorder identified by Kraepelin, including an unusual form of amnesia. After her death, Alzheimer examined her brain and discovered unusual plaques and tangles. These are the classic identifiers of the disease, which could only be diagnosed post-mortem with an autopsy, until the end of the twentieth century. After Kraepelin and Alzheimer's identification of the disease in the early twentieth century, the Alzheimer's history showed that not many advances were made in understanding or treating the disease. The name of Alzheimer's disease only gained popularity in the 70s and 80s as a label for patients over the age of 65. Now the disease has recognizable and diagnosable symptoms, which can appear in patients as young as 30. Typically, an aggressive type of Alzheimer's disease that occurs in patients under the age of 65 has a known genetic factor, while the appearance of the disease in patients over 65 has a number of other factors in regards to its development, such as health, occupation, and environment.

Alzheimer described a 'peculiar substance' occurring as extracellular deposits in specific brain regions, which are now referred to as amyloid plaques. It was not until the mid-1980s that it was discovered that the plaques consist of aggregates of a small peptide called amyloid- β ($A\beta$) (Masters et al. 1985). $A\beta$ is produced by endoproteolysis of the parental amyloid precursor protein (APP), which is achieved by the sequential cleavage of APP by groups of enzymes or enzyme complexes termed α -, β - and γ -secretases (Fig.2) (Flank et al. 2007).

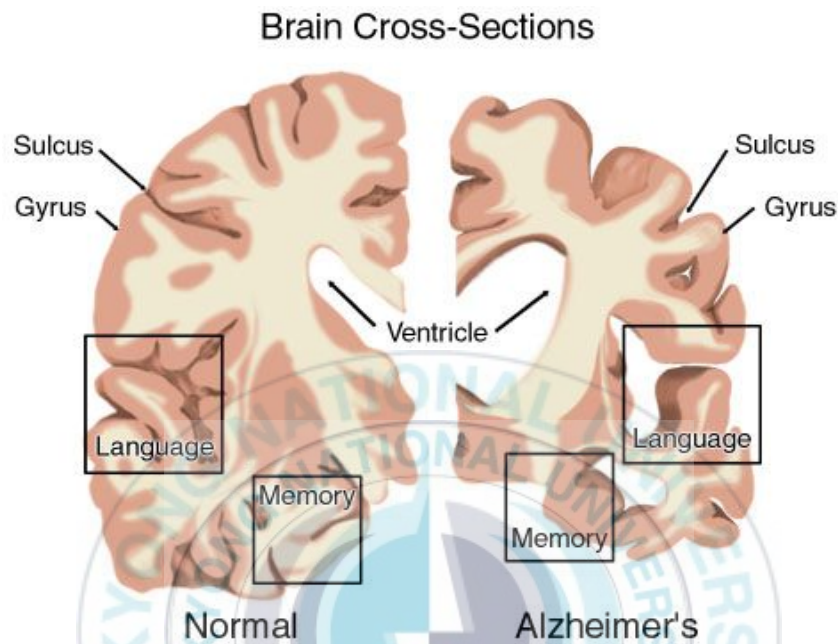


Figure 1. These images represent a cross-section of the brain as seen from the front. The cross-section on the left represents a brain from a normal individual and the one on the right represents a brain with Alzheimer's disease. In the early stages of Alzheimer's disease, short-term memory begins to decline when the cells in the hippocampus degenerate. As Alzheimer's disease spreads through the cerebral cortex, judgment declines, emotional outbursts may occur and language is impaired. Progression of the disease leads to the death of more nerve cells and subsequent behavior changes. The ability to recognize faces and to communicate is completely lost in the final stages. Patients lose bowel and bladder control, and eventually need constant care.

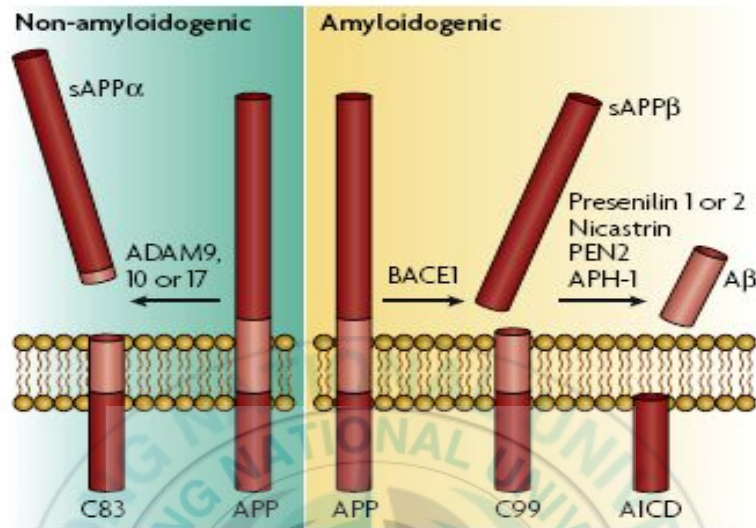


Figure 2. The A β peptide is derived via proteolysis from a larger precursor molecule called the amyloid precursor protein (APP). APP can undergo proteolytic processing by one of two pathways. Most is processed through the non-amyloidogenic pathway, which precludes A β formation. The first enzymatic cleavage is mediated by α -secretase. Cleavage by α -secretase occurs within the A β domain, thereby preventing the generation and release of the A β peptide. Two fragments are released, the larger ectodomain (sAPP α) and the smaller carboxy-terminal fragment (C83). Furthermore, C83 can also undergo an additional cleavage mediated by γ -secretase to generate P3 (not shown). APP molecules that are not cleaved by the non-amyloidogenic pathway become a substrate for β -secretase (β -site APP cleaving enzyme 1; BACE1), releasing an ectodomain (sAPP β), and retaining the last 99 amino acids of APP (known as C99) within the membrane. The first amino acid of C99 is the first amino acid of A β . C99 is subsequently cleaved 38–43 amino acids from the amino terminus to release A β , by the γ -secretase complex.

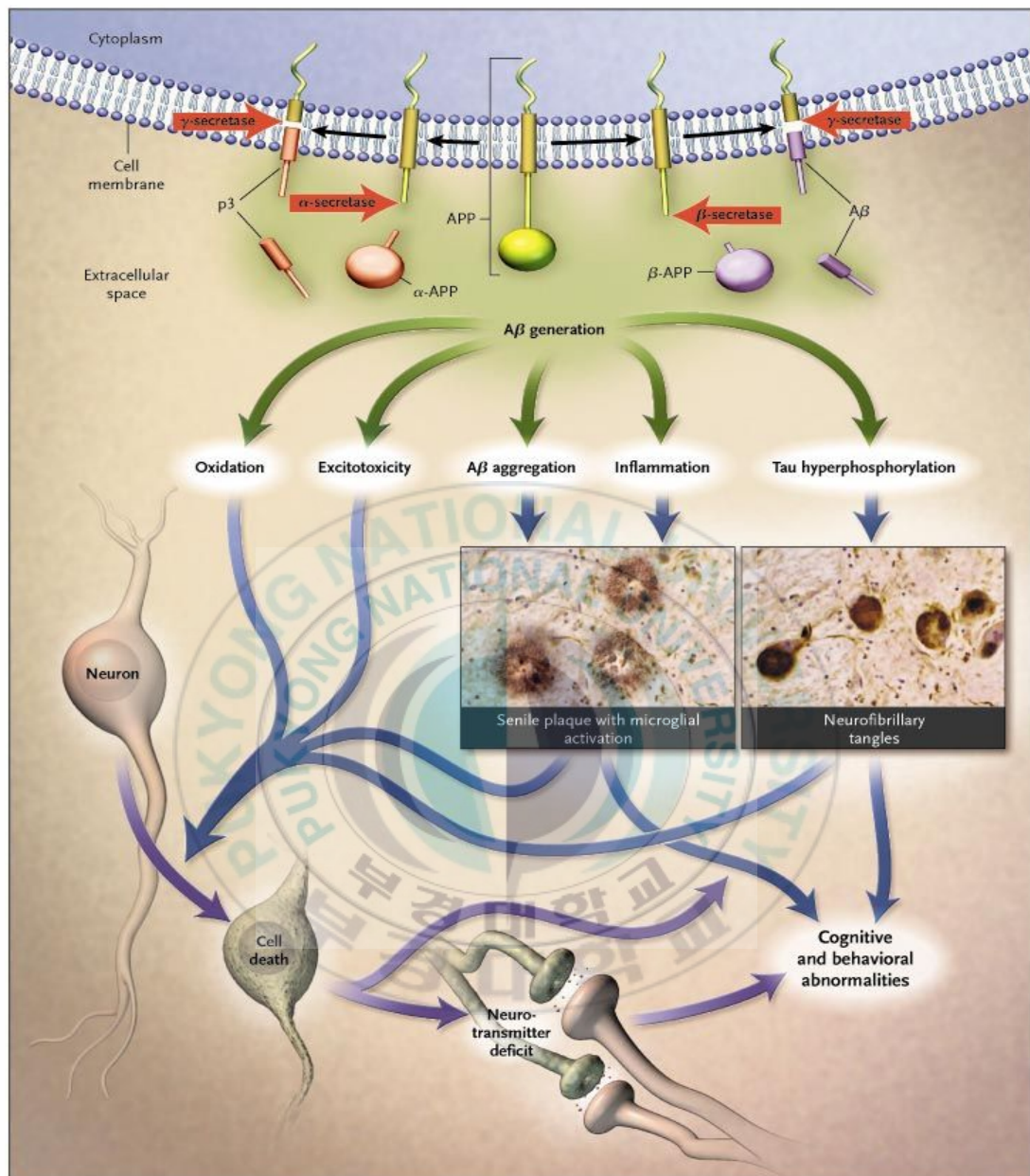


Figure 3. Putative Amyloid Cascade. This hypothesis of the amyloid cascade, which progresses from the generation of the A β peptide from the amyloid precursor protein, through multiple secondary steps, to cell death, forms the foundation for current and emerging options for the treatment of Alzheimer's disease.

Oxidative stress reflects a situation wherein reactive oxygen species (ROS), such as free radicals and their products, are in excess of the antioxidant defense systems. The link between the amyloid deposits and oxidative stress in AD brain is not readily apparent due to the fact that studies of postmortem tissue cannot reveal whether these deposits are the byproducts of neurodegeneration or precede the degenerative process (Fig. 3). However, there is increasing evidence shows that A β itself is associated with oxidative stress. Several markers of excess oxidative stress, such as an increase in ROS, accumulation of oxidized products serve to establish the direct role of A β in the oxidative damage associated with AD (Varadarajan et al. 2000). The A β -associated accumulation of ROS result in damage to major components of cells: nucleus, mitochondrial DNA, membranes, and cytoplasmic proteins. Free radicals are in fact potent deleterious agents causing cell death or other forms of irreversible damage (Ames et al. 1991). Neurons appear to be particularly vulnerable to attack by free radicals for the following reasons: 1) their glutathione content, an important natural antioxidant, is low (Cooper et al. 1997); 2) their membranes contain a high proportion of polyunsaturated fatty acids (Hazel et al. 1990.); and 3) brain metabolism requires substantial quantities of oxygen (Smith et al. 1995.).

The fact that age is a key risk factor in AD provides considerable support for the free radical hypothesis because of effects of the attacks by free radicals. Free radicals are involved in many kinds of age-related pathologies, specifically in AD and all neurodegenerative disease (Beal et al. 1997). Although normal individuals have special mechanisms (antioxidants) that protect them from the harmful effects of ROS, Alzheimer's patients have reduced tolerance for oxidative stress. The brains from Alzheimer's patients show higher levels of oxidative damage than age matched controls. Oxidative stress may contribute to the neuronal degeneration observed in a wide variety of neurodegenerative disorder of the central nervous system and pathological condition such as ischemia and trauma brain injury (Frances et al. 1999). Especially, frailty of

the brain to oxidative stress is related to its high rate of oxygen consumption, being oxidation damage detrimental to neurons. The oxidation of mitochondrial DNA and, to a lesser extent, of nuclear DNA has been observed in the parietal cortex of AD patients (Mecocci et al. 1994). Protein oxidation has also been observed in elderly individuals with and without AD, but appears to be more marked in AD patients in the regions presenting the most severe histopathologic alterations (Hensey et al. 1995). Many studies have shown increased lipid peroxidation in the brains of AD patients. Lipid peroxidation is a major cause of depletion of membrane phospholipids in AD. One of the products of lipid peroxidation, 4-hydroxynonenal, which is found in high concentrations in AD patients (Markesbery et al. 1998), proved to be toxic to hippocampal cells in culture (Mark et al. 1997).

Because $A\beta_{25-35}$ generates ROS, $A\beta_{25-35}$ can induce apoptotic cell death related with ROS in a variety of mammalian cell types in vitro. These findings raise the possibility that $A\beta$ may be responsible for apoptotic cell death observed in the brains of AD patients. From many studies in non-neuronal cell types, particularly in fibroblasts and epithelial cells, a key role for p53 as regulator of apoptotic cell death has been inferred (Ding et al. 1998). In particular, the activation of p53 in response to various stress stimuli leads to increased expression of several pro-apoptotic genes (Fig. 5). Circumstantial evidence suggests that p53 may also play a role in apoptotic death occurring in the brain of AD patients. Thus, it was shown that p53 expression is increased in the brain of AD patients and in the brain of $A\beta$ transgenic mice (LaFerla et al. 2007).

The bcl-2 family, a group of apoptosis regulatory genes, has received particular attention. In this family, bcl-2 and bcl-xL are anti-apoptotic factors, whereas bax, bcl-x, bad, bak, and bik are pro-apoptotic ones. Dimerization of anti-apoptotic factors with pro-apoptotic factors is assumed

to be a critical interaction. For example, cells continue to survive if bcl-2 predominates over bax. In contrast, a higher concentration of bax compared with Bcl-2 enhances cell susceptibility to apoptosis (Oltvai et al. 1993).

The execution of neuronal apoptosis involves relatively few pathways that converge on activation of the cysteine proteases called caspases (Friedlander. 2003). To date, 14 caspases have been identified in mammals. Two principal pathways are well-known with respect to their activations: the cell surface death receptor pathway and the mitochondrial pathway. In the death receptor pathway, activation of caspase-8 is the critical event that transmits the death signal (Fig. 6). In the mitochondrial pathway, caspase activation is triggered by the formation of an apoptotic protease-activating-factor-1 (Apaf-1)/cytochrome c complex that is fully functional in recruiting and activating procaspase-9. Activated caspase-9 then cleaves and activates downstream caspases, such as caspase-3, -6, and -7. The mitochondrial pathway appears to be regulated by the Bcl-2 family of proteins, and there may be participation of ion channels/nonselective pores, in particular the permeability transition pore (PTP), that may be activated by pro-apoptotic stimuli. Accumulating evidence implicates selective neuronal loss in neurodegenerative diseases, including AD, which involves activation of these caspases (Takuma et al. 2005) (Fig. 7).

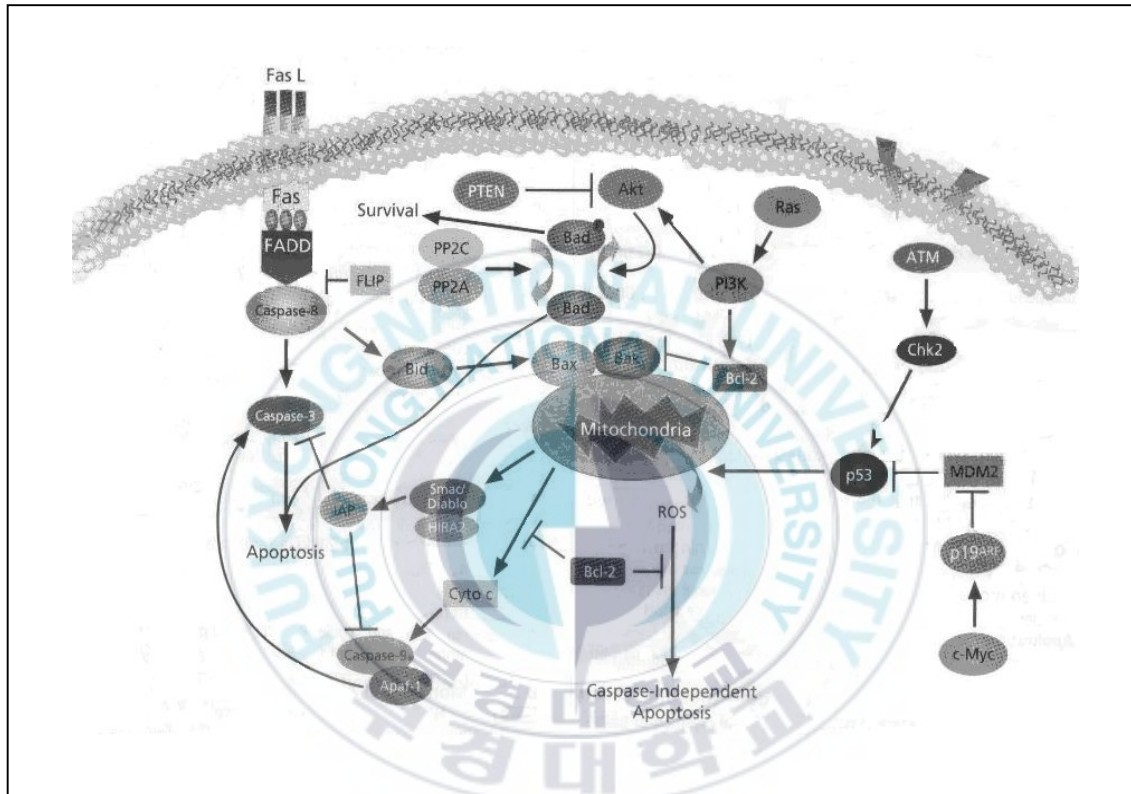


Figure 4. Activation and inhibition of apoptosis. Several mechanisms have been identified in mammalian cells for the induction of apoptosis. These mechanisms include factors that lead to perturbation of the mitochondria leading to leakage of cytochrome c or factor that directly activate members of the death receptor family.

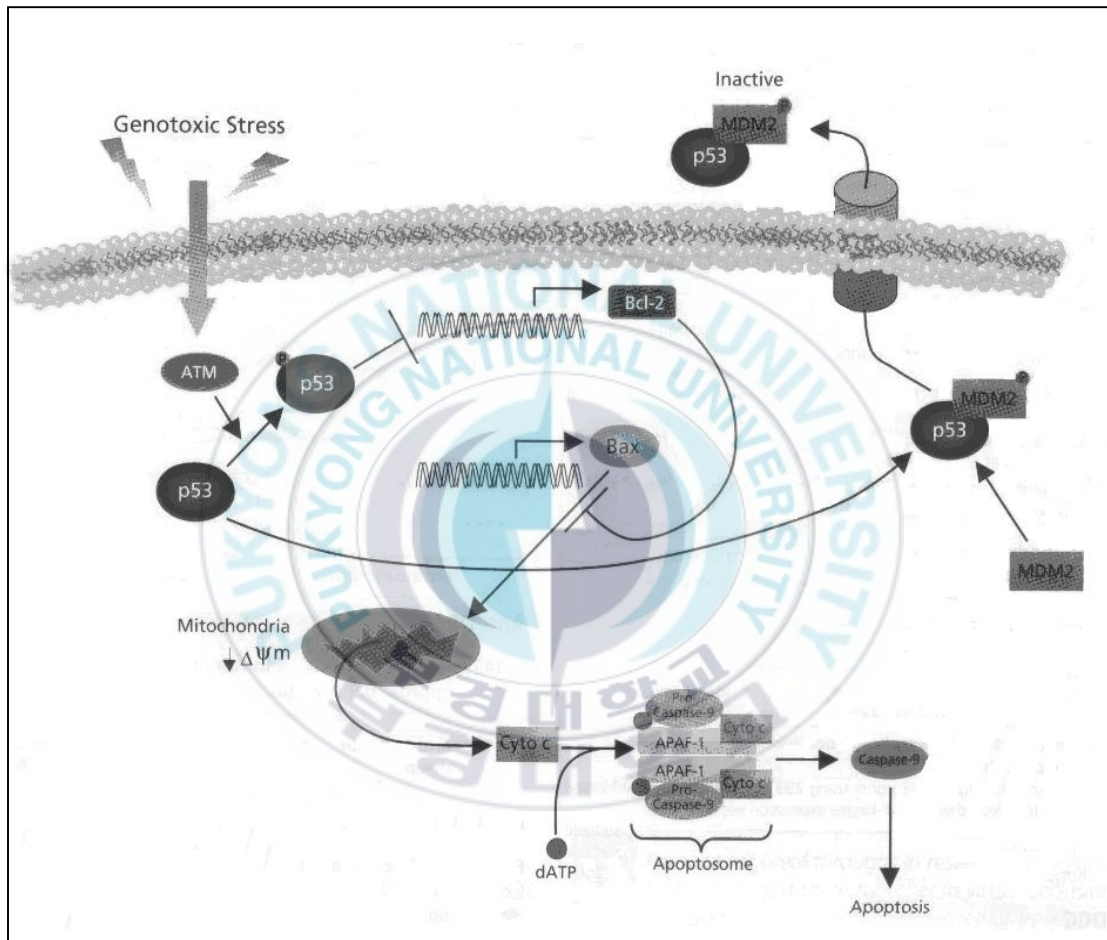


Figure 5. p53 signaling pathway. P53 can cause growth arrest of the cell at a checkpoint to allow for DNA damage repair or can cause the cell to undergo apoptosis if the damage cannot be repaired.

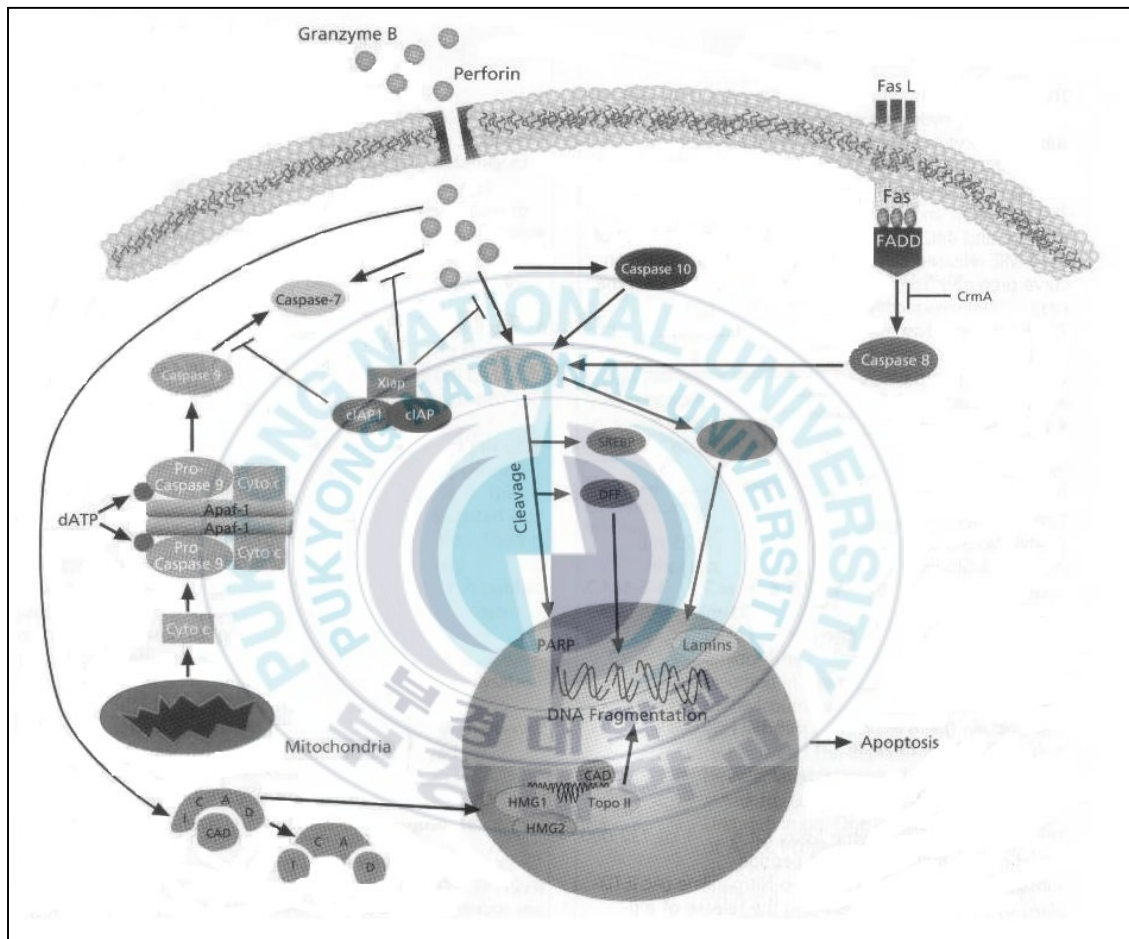


Figure 6. Caspase Cascade. Apoptosis or programmed cell death is triggered by a variety of stimuli, including cell surface receptors, the mitochondrial response to stress. The caspases comprise a class of cystein proteases, many members of which are involved in apoptosis. The caspases convey the apoptotic signal in a proteolytic cascade, with caspases cleaving and activating other caspases that in turn activate enzymes that subsequently degrade cellular targets that lead to cell death.

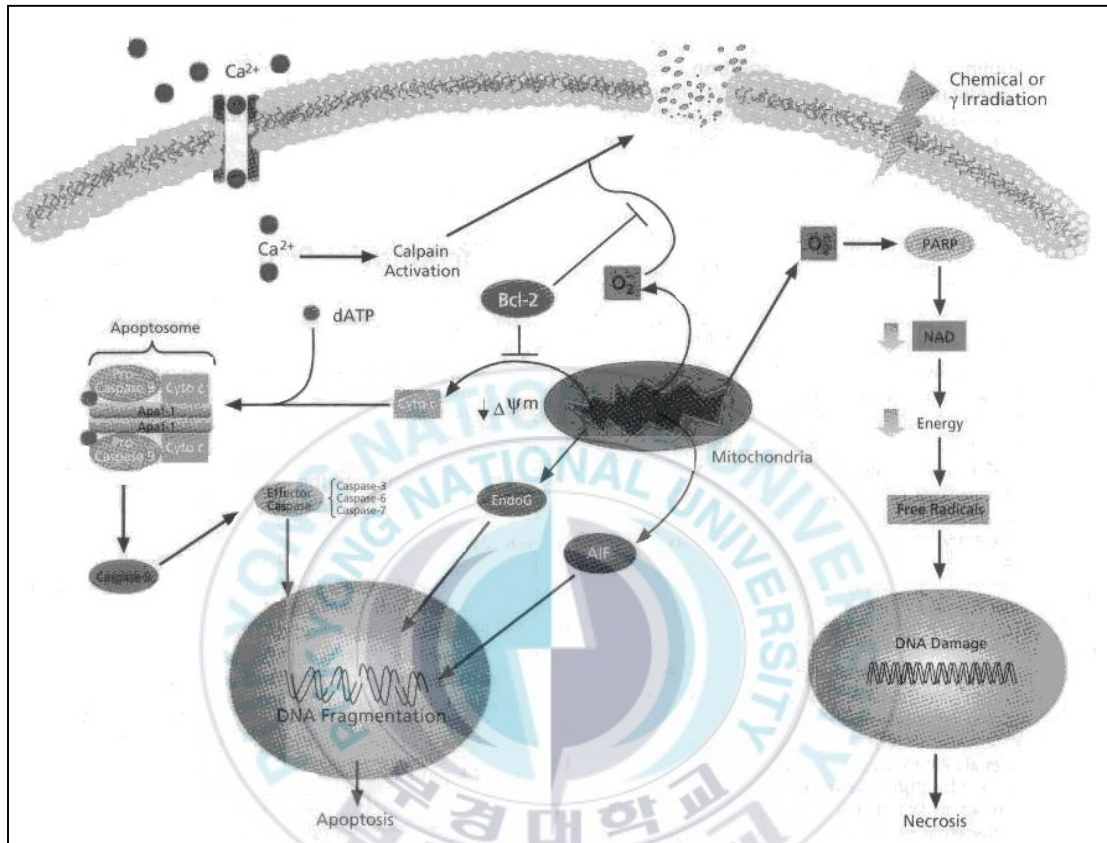


Figure 7. Oxidative damage due to the endogenous production of reactive oxygen species by mitochondria can lead to cell death via apoptosis. Two such factors, cytochrome c and apoptosis inducing factor (AIF), begin a cascade of proteolytic activity that ultimately leads to nuclear damage (DNA fragmentation) and cell death. Cytochrome c, a key protein in electron transport, appears to act by forming multimeric complexes with Apaf-1, a protease, which in turn activates pro-caspase-9, and begins a cascade of activation of downstream caspases. Bcl-2 and Bcl-x can prevent pore formation and block the release of cytochrome c from the mitochondria and prevent activation of caspase cascade and apoptosis.

Few studies have assessed apoptosis morphologically in AD neurons. In those that have, neurons are not necessarily shrunken, the chromatin is not compacted, membrane blebbing is not observed and there is preservation of organelle structural integrity. The nuclei are often swollen rather than pyknotic. Some reports indicate the increase in neurons containing condensed nuclear DNA and no nucleolus in AD.

DNA fragmentation in apoptotic cells is the result of the activation of deoxyribonucleases (DNases) that cleave the genomic DNA at regular intervals. While there is no strong evidence for apoptotic morphology in AD neurons, there is some evidence that DNA fragmentation is increased in AD. As early as the 90's, it has been shown that there is a 2 fold increase in DNA breaks in AD. Using various techniques to label the 3' ends of the fragmented DNA, several investigators have seen an increase in DNA fragmentation in the hippocampus and the entorhinal cortex, in the temporal cortex, and insular and midfrontal gyrus. The amount of labeled cells is significantly different from normal controls. The cell types with fragmented DNA are not always assessed but some studies have shown DNA fragmentation in glia with only 28% in neurons whereas other claims that all positive cells are neurons. The fact that cells with fragmented DNA have swollen nuclei indicates that the cell death observed is necrotic rather than apoptotic. However, as stated above, it does not rule out an apoptotic mechanism for the initial cell death that cannot be detected in late AD.

It has recently been suggested that endogenous factors, such as acetylcholinesterase (AChE) play significant roles in modulating the cytotoxicity of A β (Alvarez et al. 1998). In the AD brain, AChE is associated predominantly with the amyloid core of mature senile plaques, diffuse "pre-amyloid" deposits, and the endothelial lining cerebral blood vessels. More relevantly, the brain areas where senile plaques are present are strongly AChE positive (Calderon et al. 1998). AChE also directly promotes assembly of A β peptide into amyloid fibrils, whose toxicity is higher than

that of the A β aggregates alone (Alvarez et al. 1998). Since such findings have suggested that there is close interaction between AChE and A β , it has become of interest to know the role of AChE activity in A β - induced apoptosis (ZHANG et al. 2003).

Chitin, a polymer of *N*-acetylglucosamin (β -1,4-glucosidic linkage of 2-cetoamino-D-glucose), is a cellulose-like biopolymer present in the exoskeleton of crustaceans, in the cuticle of insects, and also in the cell wall of some fungi, microorganism, and yeast. Chitin is a water-insoluble material resembling cellulose in its solubility. Chitosan is derived from chitin by deacylation in the presence of alkali. Therefore, chitosan is copolymer consisting of β -(1 \rightarrow 4)-2-amino-D-glucose units with the latter usually exceeding 80% and water soluble by making salt with various acids on the amino groups of D-glucosamine units. Additionally, partially acetylated chitosan having about 50% D-glucosamine units is only able to dissolve in water (Aiba, 1989). The structure of chitin and chitosan are shown in Fig.8.

Until the middle of the 1980s, major applications of chitosan were centered on sludge dewatering, food processing, and metal ion chelation. Recently, new applications, however, are concentrated on producing high valuable products by means of cosmetics, drug carriers, food additives, semi-permeable membranes, and pharmaceuticals. Chitosan have been developed as new physiologically bioactive materials since they possess various biological activities such as antihypertensive activity (Okuda et al. 1997), antibacterial activity (Allan et al. 1979; Hadwiger et al. 1980; Walker-Simmons et al. 1983; Hirano et al. 1989; Uchida et al. 1989; Jeon et al. 2000; Kim et al. 2000), and hypocholesterolemic activity (Maezaki et al. 1993; Sugano et al. 1980). In the recent studies, it has been more of interest for converting chitosan to their oligosaccharides. Even though chitosan is known to have very interesting functional properties in many areas, their high molecular weights and high viscosity restrict the uses in vivo.

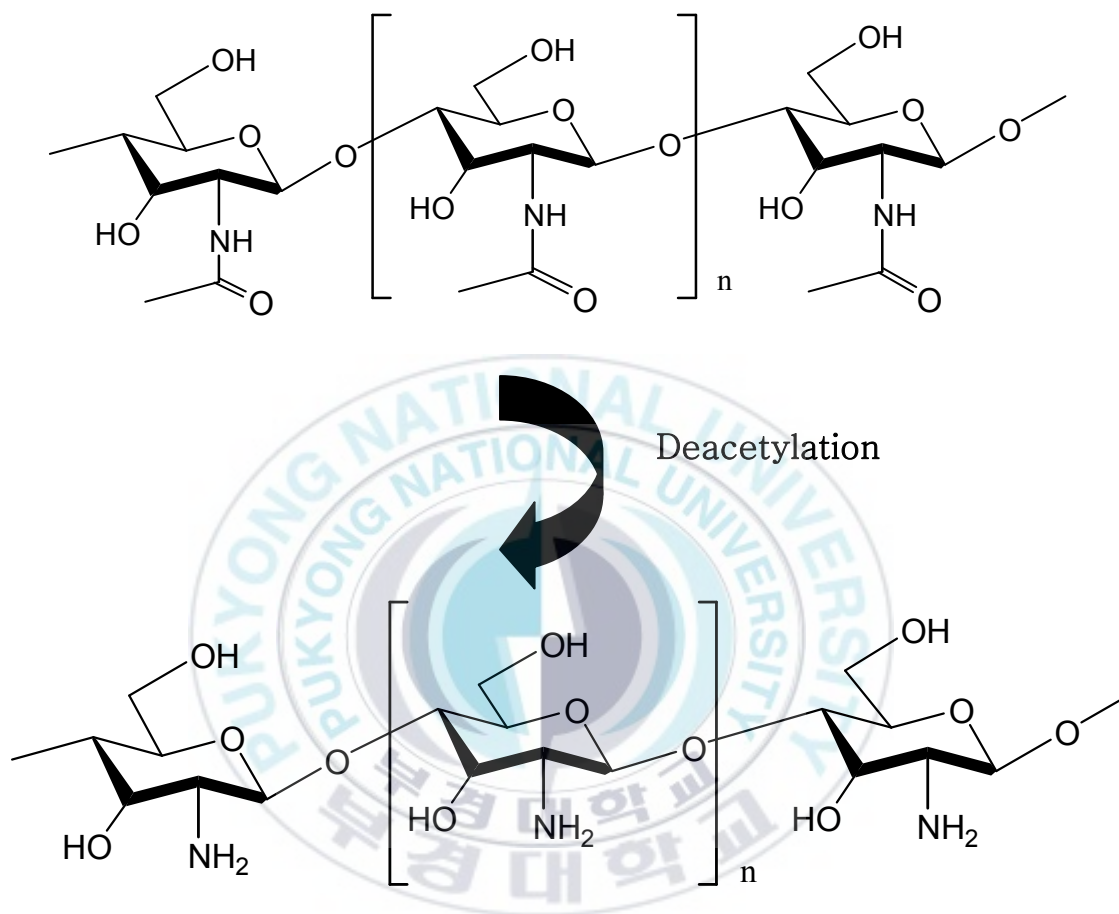


Figure 8. Structures of Chitin and Chitosan

In addition, there is little doubt that such properties will influence absorption in the human intestine. Therefore, the actions of chitosan in vivo still remain ambiguous as the physiological functional properties because most animal intestines, especially the human gastrointestinal tract, do not possess enzyme which digest on the β -glucosidic linkage in chitosan (Weiner 1992) and consequently the unbroken polymers may be poorly absorbed into the human intestine. However, chitosan is water-insoluble, high molecular size, and more difficult to absorb to body. Especially, most animal intestines including human gastrointestinal tract do not possess enzymes which digest on the β -glucosidic linkage in chitosan, resulting that are exerted unchanged in the feces without any degradation of significant absorption. In the recent studies, it has been more of interest for converting chitosan to their oligomers. Even though chitosan is known to have interesting functional properties, direct absorption is difficult in the intestine of human because of physicochemical properties of chitosan.

Chitooligosaccharides (COS) is hydrolyzed derivative of chitosan and has lower viscosity, relatively small molecular sizes, and short chain lengths, and is soluble in neutral aqueous solution. Subsequently, they seem to be readily absorbed in vivo system. They also possess additional functional properties such as antitumour activity (Suzuki et al. 1986; Tsukada et al. 1990; Jeon et al. 2002), enhancing protective effects against infection with some pathogens associated in mice (Yamada et al. 1993; Tokoro et al. 1989), antifungal activity (Hiroan et al. 1989), and antimicrobial activity (Allan et al. 1979; Kim et al. 2000; Jeon et al. 2001).

Because it is expected that COSs are absorbed and possess bioactivity in the in vivo system, using of COS is more efficient than that of chitosan. This study was focused on the effect of COS. As mentioned above, COS possess many kinds of functions however there is little information of bioactive properties on Alzheimer's diseases. Pc-12, derived from rat pheochromocytoma, is useful for studying ability of neuron cells. The aim of this study,

therefore, was to investigate not only inhibitory effect of apoptotic cell death induced by A β but also inhibitory effect of AChE using pc-12 cell (rat pheochromocytoma) line.



Experimental procedure

1. Materials

Different molecular weight of chitooligosaccharides (COS) were donated by Kitto Life Co. (Seoul, Korea). Pc-12 cell lines (pheochromocytoma; adrenal gland) were obtained from Korean Cell Line Bank (Seoul, Korea). Cell culture medium (DMEM F-12), Trypsin-EDTA, penicillin/streptomycin, fetal bovine serum (FBS), and other materials required for culturing cells were purchased from Gibco BRL, Life Techniligy (NY, USA) and Sigma Chemical Co. (St. Louis, MO, USA). MTT reagent (3-(4,5-dimethyl-2-yl)-2,5-diphenyltetrazolium bromide), Acetylthiocholine (ATCh), 5,5'-dithiobis-(2-nitrobenzoic acid) (DTNB), propidium iodide, RNase, Proteinase K, ethidium bromide and dithiothreitol (DTT) were purchased from Sigma Chemical Co. (St. Louis, MO, USA). 2',7'-Dichlorofluorescein diacetate (DCFH-DA) was obtained from Molecular Probe Inc., (OR, USA). TUNEL assay kit was purchased from Invitrogen (CA, USA). Beta-amyloid (A β) was synthesized by Peptron Inc. (Dae-jeon, Korea). Primary and secondary antibodies used for western blot analysis were purchased from Santa Cruz Biotechnology (CA, USA). Trizol® was obtained from Invitrogen (CA, USA) and AMV reverse transcriptase was purchased from USB Corporation (OH, USA).

2. Preparation of chitosan oligosaccharides using an UF membrane bioreactor

Crab shell wastes are currently utilized as the major industrial source of biomass for the large-scale production of COS. These crustacean shell wastes are composed of protein, inorganic salts, chitin and lipids as main structural components. Therefore, the extraction of chitin and chitosan (the starting material of COS) is mainly employed stepwise chemical

methods. In the first step, crab shells are treated with 3-5% aqueous NaOH solution to remove protein attached to the shells and thereby prevent the contamination of chitin products with proteins. Deproteinized shells are then neutralized and calcium is removed by treating with 3-5% aqueous HCl solution to afford a white or slightly pink precipitate of chitin. Then the chitin is *N*-deacetylated with 40-45% NaOH to form chitosan with a cationic nature. The resulting crude sample is dissolved in 2% acetic acid and the supernatant is neutralized with aqueous NaOH solution to afford purified chitosan as a white precipitate (Hirano, 1996). After alkaline deacetylation, some of the amino groups may remain acetylated and distribute randomly along the whole polymer chain.

Chitosan oligosaccharides were prepared by continuous hydrolysis of chitosan in a UF (ultra-filtration) membrane reactor system connected to an immobilized enzyme column reactor in which chitosanase from *Bacillus sp.* was absorbed on chitin as a carrier for immobilization, according to our previous method (Jeon et al., 2000). A 1% chitosan solution was prepared by dispersing chitosan in with ratio 1L of water, dissolving it and stirring by adding 400 ml of 1M lactic acid and make up to 15 L with water; the pH was adjusted to be 5.5 with a saturated NaHCO₃ solution. The chitosan was hydrolyzed by enzymatic reaction in the reactor system and fractioned by passing through UF membrane of molecular weight cut-off (MWCO) 10 kDa, 5 kDa, 3 kDa, and 1 kDa.

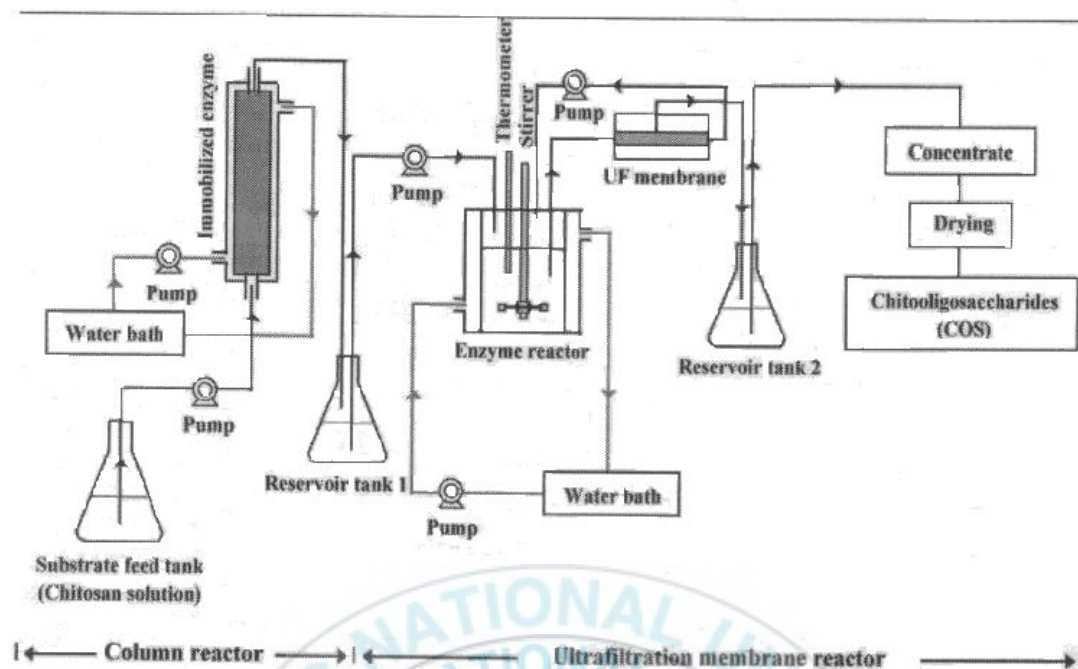


Figure 9. Schematic diagram of the dual reactor system developed for continuous production of chitooligosaccharide (COS).

Adapted from Jeon and Kim (2000)

3. Sample preparation

1g of each molecular weight of COS was dissolve in 10ml DMEM F-12 absence fetal bovine serum make 10,000 $\mu\text{g/ml}$ of stock solution. Stock solutions were sterilized by filter through 0.22 μm sterilized filter. From 10,000 $\mu\text{g/ml}$ of stock solution, sample with different concentrations were prepared in DMEM F-12 absence fetal bovine serum. After that, samples were stored at 4 $^{\circ}\text{C}$. pH of sample were measured in order to show effect on pH of cell cultured media.

4. Cell Culture

Pc-12 cells were cultured in 10 cm^2 tissue culture plate (SPL Lifesciences, Korea) and maintained in Dulbecco's Modification of Eagle's Medium F-12 (DMEM F-12) supplement

with 10% fetal bovine serum (FBS), and 100 µg/ml penicillin-streptomycin and maintained at 5% CO₂ and 37 °C humidified atmosphere. Pc-12 cells were detached with trypsin-EDTA on culture dishes, 24- or 96- well plate and used for experiment at about 70-80 % confluency.

5. Cell viability (MTT assay)

Cytotoxicity levels of COS on pc-12 cells were measured using MTT method. The cells were grown in 96-well plates at a density of 1×10^4 cells/well. After 24 h, cells were treated with different concentrations of COS and after 1 h, some chemicals were added. After 24 h of incubation, 100µl of MTT solution (1mg/ml) was added and incubated for 4 h. Finally, 100µl of DMSO was added to solubilize the formazan salt formed and amount of fomazan salt was determined by measuring the optical density (OD) at 540nm using a GENios microplate reader (Tecan Austria GmbH, Austria). Relative cell viability was determined by the amount of MTT converted to formazan salt. The percentage of viable cells compared to the control was calculated as a percentage (OD of treated cells / OD of blank \times 100) and dose response curves were developed. The data were expressed as mean from at least three independent experiments and $P < 0.05$ was considered significant

6. Acetyl cholinesterase (AChE) inhibitory activity

Ellman assay was used to evaluate the inhibitory activity of AChE. When Acetylthiocholine (ATCh), as a substrate, is hydrolysed, thiocholine is formed. This thiocholine is reacted with 5,5'-dithiobis-(2-nitrobenzoic acid) (DTNB) and then, this compound form dithio complex and 5-thio-2-nitrobenzoate. In this experiment, A β was added to the pc-12 cell line for 24 h to stimulate AChE and cell lysates are used as a AChE. We used Sodium phosphate buffer (pH8.0) and the concentration of ATCh and DTNB are 0.5mM. The wavelength of absorbance is 412nm.

(ul)	Blank1	Blank2	Control	Sample
Buffer	180	160	160	140
Sample	X	20	X	20
Enzyme	X	X	20	20

$\xrightarrow{25^{\circ}\text{C}, 30\text{min}}$ DTNB: 10ul
ATCh: 10ul

3min 40sec

\downarrow
O/D 412nm

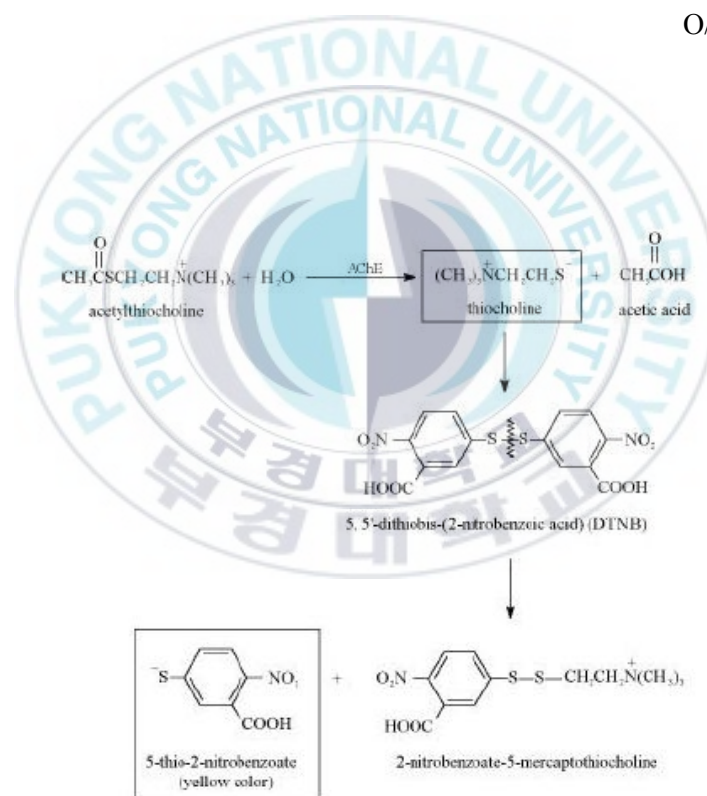


Figure 10. Ellman's assay for determination of AChE activity

7. Cellular ROS determination by Dichlorofluorescein diacetate (DCFH-DA)

Oxidation-sensitive dye DCFH-DA was used to detect formation of intracellular reactive oxygen species (ROS). For this experiment, pc-12 cells growing in fluorescence microtiter 96-well plates were labeled with 20 μ M DCFH-DA in HBSS for 30 min in the dark. Cells were then treated with different concentrations of COS and incubated for 24 h. After washing the cells with PBS for three times, 25 μ M A β ₂₅₋₃₅ was added. The intensity of fluorescence signal emitted by 2',7'-dichlorofluorescein (DCF) due to oxidation of DCFH by cellular ROS was detected time dependently ($\lambda_{\text{excitation}} = 485 \text{ nm}$, $\lambda_{\text{emission}} = 528 \text{ nm}$) using a GENios[®] fluorescence microplate reader. Following maximum rate of fluorescence increase, each well was normalized to cell numbers using MTT cell viability assay. Effects of treatments were plotted and compared with fluorescence intensity of control and blank groups.

8. Fluorescence microscopy analysis

Treated cells were visualized following acridine orange staining method. Cells were cultured in appropriate media at a density of 1×10^5 cells in 6-well plate and incubated for 24h. Cells were treated with different concentrations of test materials and chemicals. Following incubation for 24h, cells were stained with 40 μ l of a mixture of acridine orange (100 mg/ml) and ethidium bromide (100 mg/ml) in cultured medium, and immediately examined under a fluorescence microscope and images were recorded using a connected digital camera (Olympus C5050, Tokyo, Japan).

9. Terminal deoxynucleotidyl transferase biotin-dUTP nick end labeling (TUNEL) assay

Pc-12 cells culturing in 6 well plates were treated with different concentrations of COS and

A β . After 24 h TUNEL assay was employed to identify apoptotic cells having free 3'-OH of cleaved DNA using kit (TUNEL apoptosis detection kit, Upstate cell signaling solutions, NY, USA) according to manufacturer's instructions. Briefly, treated cells were washed twice with PBS and fixed with 0.5% glutaraldehyde in PBS for 15 min. Following washing cells three times with PBS cells were incubated with a solution containing 0.05% tween, 0.2% BSA in PBS for 15 min at room temperature. After washing, free 3'-OH of cleaved DNA in apoptosized cells was labeled by incubating for 60 min with Terminal deoxynucleotidyl transferase (TdT) end labeling cocktail containing Tdt buffer, Biotinylated deoxyuridine triphosphate (Biotin-dUTP) and TdT. Reaction was stopped by adding termination buffer (TB buffer). Cells were then washed with PBS and incubated with the blocking buffer at room temperature for 20 min. Following removal of blocking buffer, cells were incubated in dark for 30 min at room temperature with avidin-FITC solution. Since this assay is based on the detection of single and double stranded DNA breaks (nick) by using terminal deoxynucleotidyltransferase-mediated dUTP nick end labeling (TUMEL), localization of fragmented DNA was detected by fluorescent microscope (Axiovert 200, Zeiss) using Axio version 3.1 software and compared with the cells without induction of apoptosis.

10. Cell cycle analysis by flow cytometry

Normal functioning of cell cycle in the presence of test materials was tested by flow cytometry. Pc-12 cells were cultured in 10-cm² plate were treated with different concentrations of test materials and chemicals for 24h and cells were washed phosphate buffered saline (PBS) containing 5mM EDTA, after that, fixed with 70% ethanol. Fixed cells were washed with phosphate-citrate buffer and incubated with RNase A at 37°C for 30 min. Propidium iodide (PI) with final concentration of 500 μ g/ml was added and incubated for 30 min on ice bath.

Functioning of cell cycle was analyzed using XL-MCL™ flow cytometer equipped with EXPO™ 32 software (Beckman Coulter, Inc., CA, USA)

11. RNA extraction

Total RNA was extracted from pc-12 cells after treatment with test materials. For that, cells were lysed with 1ml TRIzol®. Reagent was added to a 10-cm diameter dish, and passing the cell lysate several times through a pipette. The homogenized samples were incubated for 2 minutes at room temperature. After that, the homogenized samples were transferred into microtube 0.2 ml chloroform was added into microtube and shook vigorously by hand for 15 seconds and incubated at room temperature for 2 minutes. The process was followed with centrifugation samples 12,000 rpm at 4 °C for 15 minutes. The mixture separates into a lower red, phenol-chloroform phase, an interphase, and a colorless upper aqueous phase. Transfer the aqueous phase to a fresh tube. Precipitate the RNA from aqueous phase by mixing with isopropyl alcohol following ratio 1:1. The mixture was vortexed and kept at 4 °C for 10minutes, followed by centrifugation 12,000 rpm at 4°C for 15minutes. After remove supernatant, RNA pellet was washed once with 1 ml 75% ethyl alcohol. Ethyl alcohol was removed after the sample had centrifuged 12,000 rpm at 4 °C for 15 minutes. At the end of the procedure, RNA pellet was suspended in DEPC-H₂O and stored at -80 °C until use. The purity of the RNA was established by reading the optical density of each sample at 260nm and 280nm, using GENios microplate reader (Zhang et al. 2004)

12. Real-time polymerase chain reaction (Real-time PCR)

To synthesize cDNA, an aliquot of 1.0 µg of RNA was added to RNase-free water to a final volume of 13.5µl, denaturated for 2 min at 72 °C and cooled immediately on ice. RNA was reverse transcribed in a mastermix containing 1X RT buffer, 1 mM dNTPs, 500 ng oligo (dT)15

primers, 140 U of MMLV reverse transcriptase and 40 U of RNase inhibitor for 90 min at 42 °C in an automatic Whatman thermocycler (Biometra, UK). Real-time PCR was carried out to confirm gene expression levels of p53, Bax, Bcl-2, caspase-3, caspase-9 and G3PDH mRNA. For Real-time PCR we used mastermix containing HotStarTaq Plus DNA Polymerase, QuantiFast SYBR Green PCR Buffer, dNTP Mix, SYBR Green I dye, ROX dye (Qiagen, Germany). Quantitative SYBR Green real-time PCR was performed on Rotor gene 6000 (Corbett) using the following program: 10 min at 95 °C, followed by 40 cycles of 15 sec at 95 °C, 30 s at 60 °C and 1 min at 72 °C. The reactions were carried out using 1 µl cDNA with SYBR Green PCR master mix (Qiagen, USA). The sequences of the primer for real-time PCR are depicted in Table 2. As an endogenous reference we used G3PDH. Specificity of the PCR product was confirmed by examination of dissociation reaction plots. A distinct single peak indicated that single DNA sequence was amplified during PCR. Quantitative analysis of gene expression was performed using the comparative cycle threshold (C_T) method, in which C_T is the threshold cycle number. The target genes were normalized to an endogenous reference gene (G3PDH). To indicate relative expression, we calculated using the expression $2^{-\Delta\Delta C_T}$, where $\Delta\Delta C_T = (C_{T,target} - C_{T,actin})_{treated\ sample} - (C_{T,target} - C_{T,actin})_{control\ sample}$. Each sample was tested in triplicate with quantitative PCR. The sequences of the primer for each gene are shown in Table 1.

Target	Sequence
P53	Sense: 5'-GCCATCTACAAGAAGTCACA-3'
	Antisense: 5'-GTCTTCCAGCGTGATGATG-3'
Bax	Sense: 5'-TGCAGAGGATGATTGCTGAC-3'
	Antisense: 5'- GATCAGCTCGGGCACTTTAG-3'
Bcl-2	Sense: 5'- ATACCTGGGCCACAAGTGAG-3'
	Antisense: 5'- TGATTTGACCATTTGCCTGA-3'
Caspase-3	Sense: 5'-GGACCTGTGGACCTGAAAAA-3'
	Antisense: 5'- TGATTTGACCATTTGCCTGA-3'
Caspase-9	Sense: 5'- AAGACCATGGCTTTGAGGTG-3'
	Antisense: 5'- CAGGAACCGCTCTTCTTGTC-3'
G3PDH	Sense: 5'-GTCAACGGATTTGGTCGTATT-3'
	Antisense: 5'-AGTCTTCTGGGTGGCAGTGAT-3'

Table 1. The sequences of the primer for real-time PCR

13. Western Blot assay

1×10^6 of pc-12 cells were cultured in 10 cm dishes in media without serum for 24 h, and treated with different concentrations of COS and chemicals for 24 h in media without serum. Pc-12 cells were lysed with lysis buffer containing 50 mM Tris-HCl (pH7.5), 0.4% Nonidet P-40, 120 mM NaCl, 1.5 mM $MgCl_2$, 2 mM phenylmethylsulfonyl fluoride, 80 μ g/ml leupeptin, 3 mM NaF and 1 mM DTT at 4 °C for 30 min. The total protein was extracted and 70 μ g/ml of protein were separated using a 10% SDS-polyacrylamide gel and 5% attacking gel. The resolved proteins were transferred to a nitrocellulose membrane from the gel. The nitrocellulose blots were blocking for 1 h and 30min at 37 °C using TBS-T buffer containing 0.1% Tween-20 and 3% BSA. After washing the membrane with TBS-T twice, the blots were incubated for 1 h with suitable antibodies at 25 °C. The blots were washed and visualized with enhanced chemiluminescence's detection and imagined using LAS-3000 system and protein expression was quantified by Multi Gauge V3.0 software (Fujifilm Life Science, Tokyo, Japan).

14. Measurement of total protein concentration

Total protein of cell lysate was estimated to the Lowry method modified by Peterson (1977) with bovine serum as the standard

15. Statistical analysis

All data were expressed as mean \pm standard deviation (SD). For statical analysis of significance, analysis of variance followed by student's *t*-test.

Results and Discussion

1. pH of COS and culture media

pH of COS was measured in order to investigate the effect of sample's pH on culture media. pH of COS is different depending on concentration. pH of COS is shown in Table 1. As shown in this table, high concentrations of sample have lower pH. Because the samples were used with concentration 1000 µg/ml, pH of cultured media did not have significant change when treated with samples. With this result, we could know that pH of samples does not have any effect on changing pH of cultured media. In addition, pH of samples does not have effect on cells and activity of components containing in culture media

2. Effect of COS on viability of pc-12 cells (rat adrenal pheochromocytoma)

To evaluate cytotoxicity effect of COS on pc-12 cells, MTT assay was carried out. Pc-12 cells were treated with COS at the indicated concentrations for 24 h in the absence of FBS. As shown in Fig. 11, COS did not show any cytotoxic effect on pc-12 cells even 1000 µg/ml concentration. Therefore these results suggested that COS did not have any cytotoxicity on pc-12 cells.

Samples(COS)	1~3 kDa	3~5 kDa	5~10 kDa
Concentrations (μg/ml)			
100000	5.4	5.4	5.5
50000	5.7	5.8	6.1
10000	7.1	7.1	7.0
5000	7.2	7.2	7.4
1000	7.5	7.5	7.5
500	7.5	7.5	7.5
100	7.5	7.5	7.5
50	7.5	7.5	7.5
10	7.5	7.5	7.5
Cell culture media: 7.7			

Table 2. pH of sample solution

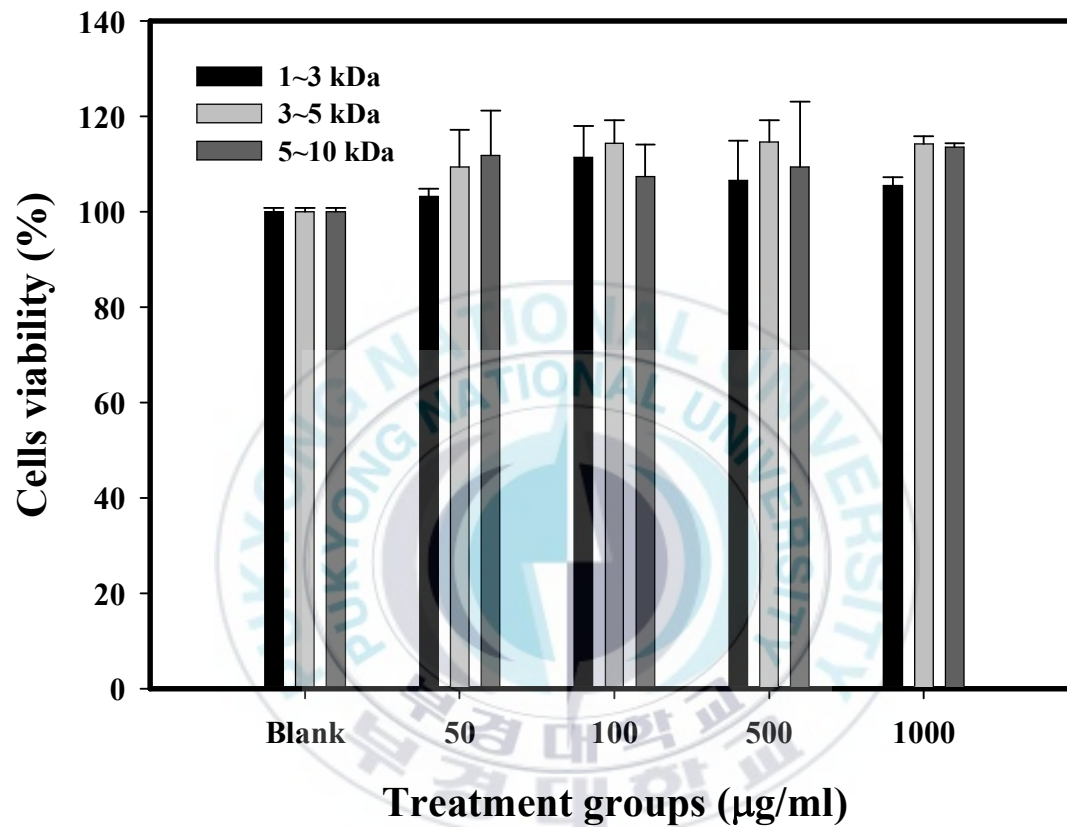


Figure. 11. Pc-12 cells (rat adrenal pheochromocytoma) were treated with COS at the indicated concentrations. Cell viability was determined by the MTT assay after 24 hours of treatment with COS. Blank: the group that was not treated with COS.

3. COS inhibited AChE activity induced by A β ₂₅₋₃₅

Measurements of cellular AChE activity after A β ₂₅₋₃₅ treatment revealed that A β ₂₅₋₃₅ stimulate AChE activity. In view of this and previous evidence that A β may interact with AChE, this experiment was performed to evaluate the A β is related to AChE expression. A β ₂₅₋₃₅ was applied to pc-12 cells that were pretreated with COS. Pretreatment with COS blocked the increase in AChE activity in dose-dependent manner (Fig. 12). In a further, to investigate the effect of COS on the AChE protein expression induced by A β , pc-12 cells were assessed for AChE protein level using appropriate antibody in the western blot experiment. Cells were treated with COS and A β (25 μ M), and then incubated for 24h. After that, total protein of cells were extracted and separated by using SDS-PAGE. The resolved proteins were transferred to a nitrocellular membrane from the gel. As shown in Fig. 13, the decrease of AChE levels were observed in dose-dependant manner.

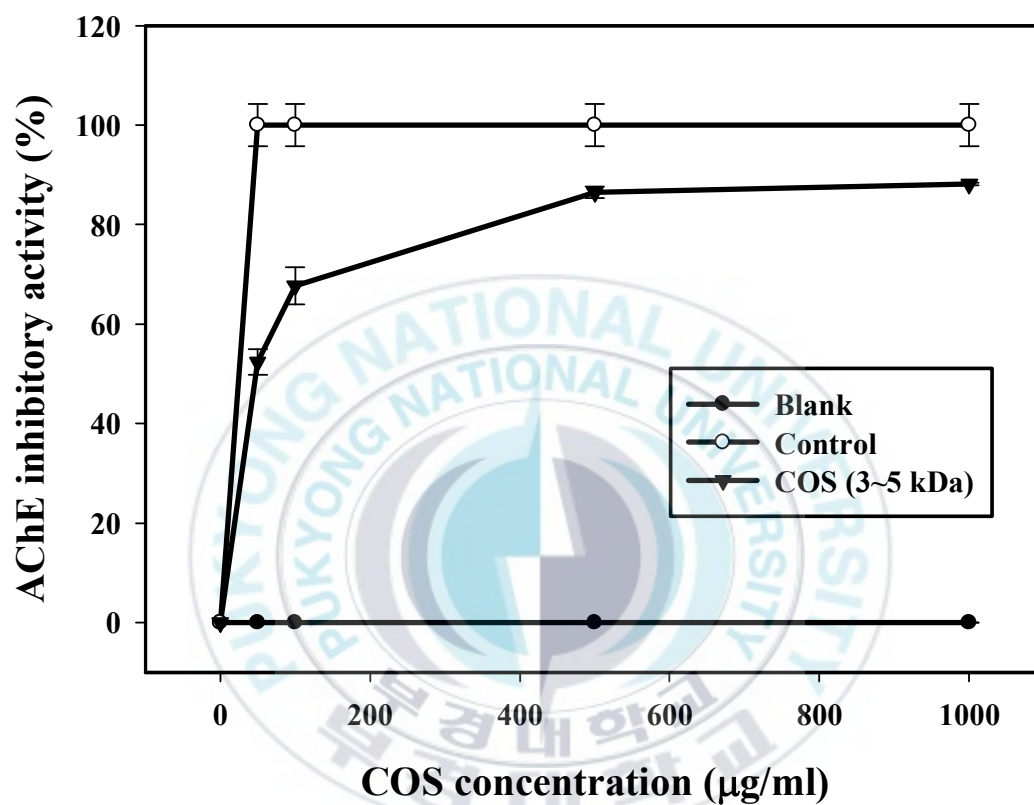


Figure 12. Measurement of AChE activity stimulated by $A\beta_{25-35}$ in pc-12 cells. Pc-12 cells were treated with 25 μ M $A\beta_{25-35}$ and incubated for 24 h. AChE activity was evaluated by Ellman assay.

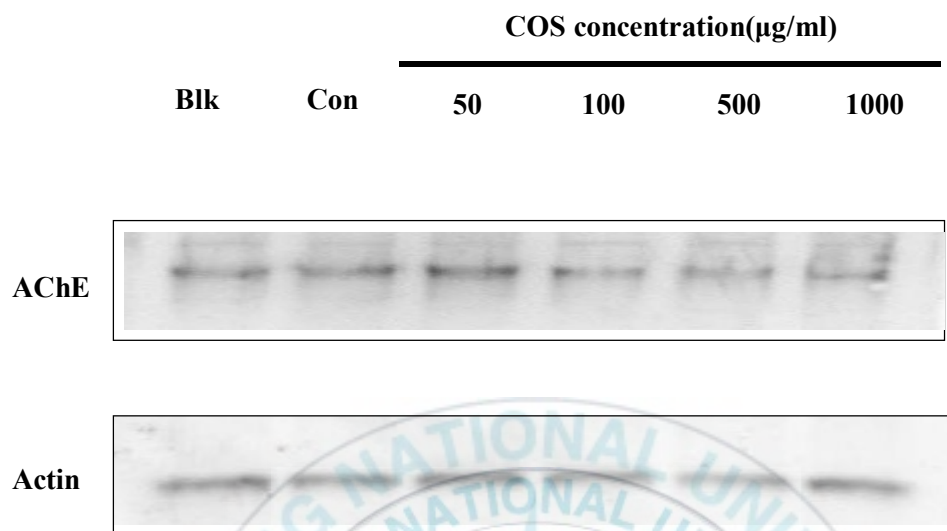


Figure 13. Western blot assay of AChE protein expression in pc-12 cells treated with COS. After treatment of COS and A β (25 μM) for 24 h, cell extracts were resolved by SDS-PAGE. Protein were transferred onto nitrocellulose membranes and incubated with antibodies. Western blot bands were developed with enhanced chemiluminescence reagents and visualized using LAS3000[®] Luminescent image analyzer. Actin was used for confirmation of equal amount of protein. Blk: non-treatment group; Con: only A β (25 μM) treatment group.

4. Effect of COS on viability of pc-12 cells affected by A β ₂₅₋₃₅

To investigate cytotoxicity effect of COS on pc-12 cells affected by A β ₂₅₋₃₅, pc-12 cells were treated with different concentrations of COS and 25 μ M A β ₂₅₋₃₅ for 24 h. As shown in Fig. 14, 3~5 kDa COS is effective to inhibit the cell death from A β ₂₅₋₃₅-induced cell death. Therefore, 3~5 kDa COS was selected for this research.

5. Effect of COS on intracellular ROS level induced by A β ₂₅₋₃₅ in pc-12 cells.

Some researchers suggested the involvement of oxidative stress in the pathogenesis of hippocampal neuronal cell death in AD (Miranda et al. 2000). By using ROS fluorescent dye, DCF, it was found that exposure of culture pc-12 cells treated with 25 μ M A β ₂₅₋₃₅ for 24 h resulted in a highly significant increase in DCF fluorescence in the cells (Fig. 15). The increase in DCF fluorescence in culture cells was essentially eliminated by cotreatment with COS (3~5 kDa). A β ₂₅₋₃₅ -induced ROS increase was almost completely inhibited by COS (3~5 kDa) in dose-dependent manner. These results suggest that COS is a potent antioxidant compound that can protect radical-mediated oxidation of cellular biomolecules.

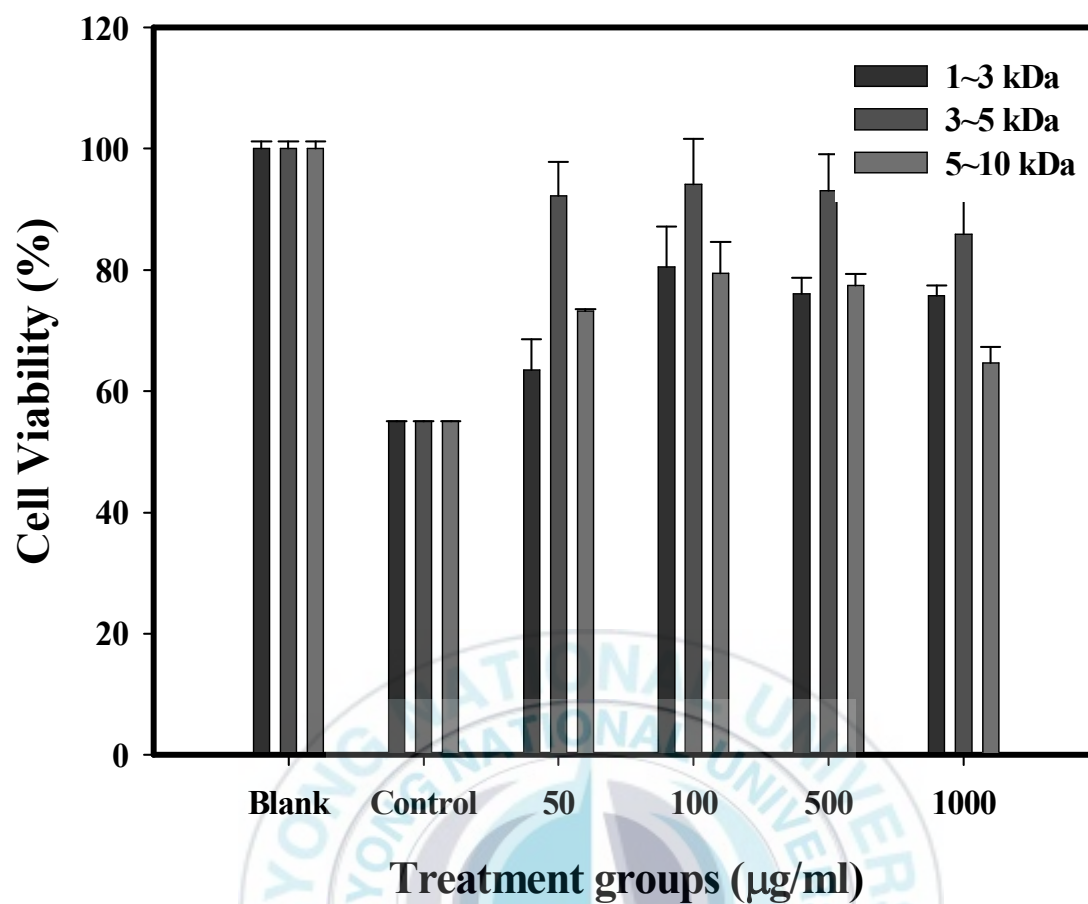


Figure 14. Pc-12 cells (rat adrenal pheochromocytoma) were treated with COS at the indicated concentrations and 25 µM A β ₂₅₋₃₅. Cell viability was determined by the MTT assay after 24 hours of treatment with COS. Blank: the group that was not treated with COS.

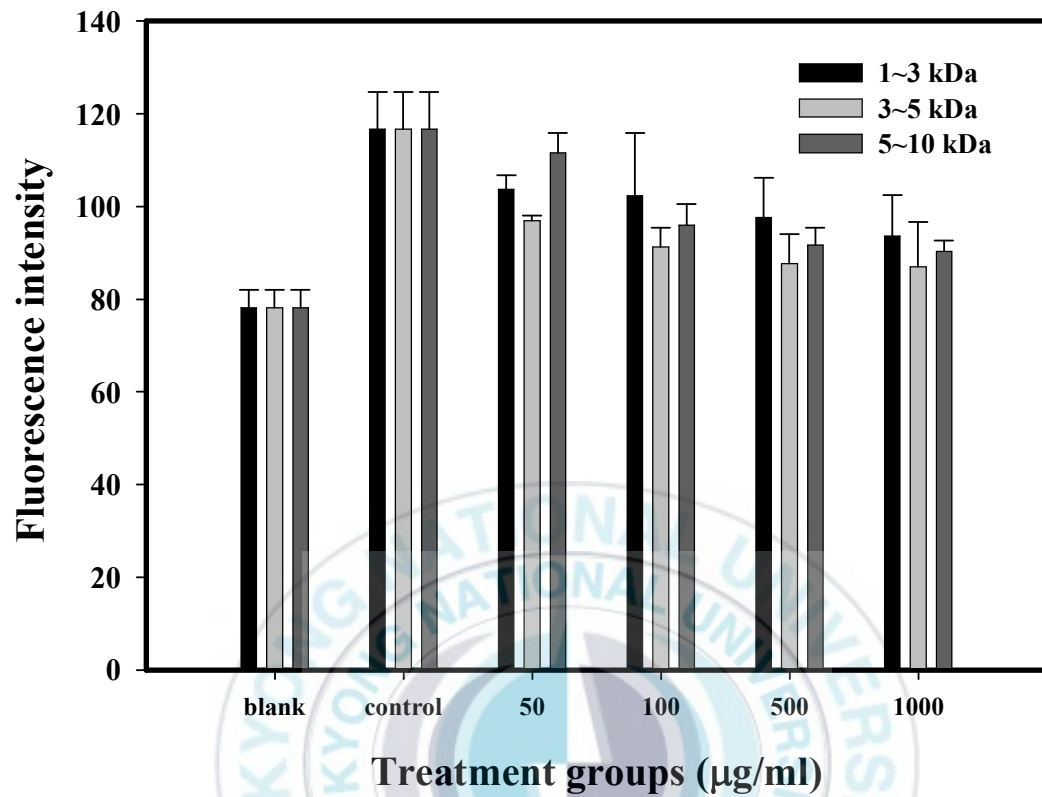


Figure 15. Cellular radical scavenging activity of COS. Pc-12 cells were labeled with non-toxic fluorescence dye, DCFH-DA, and treated with different concentrations of COS. Fluorescence intensities of DCF due to oxidation of DCFH by cellular ROS (generated $A\beta_{25-35}$) were detected time-dependently ($\lambda_{\text{excitation}} = 485 \text{ nm}$ and $\lambda_{\text{emission}} = 528 \text{ nm}$). Effects of COS on the scavenging of cellular ROS were compared with $A\beta_{25-35}$ non-stimulated blank and sample non-treated control group in three independent experiments.

6. Morphological analysis of pc-12 cells affected by A β ₂₅₋₃₅-induced apoptosis

To study cell death and morphological change, cells were visualized by staining with acridin orange and ethidium bromide. Ethidium bromide does not penetrate plasma membrane of viable cells but emits red fluorescence only after interaction with DNA of cells with damaged cell membrane. In contrast, acridine orange stain both viable and non-viable cells emitting strong green fluorescence as a result of intercalation in double-stranded DNA and red-orange fluorescence after binding with single-stranded RNA due to its accumulation in lysosomes. Fig. 16 showed the nuclear fragmentation and chromatin condensation in A β treated cells. Control group, the cells treated with only A β for 24 h, showed the strong detection of damaged cell whereas non-treated cells appeared a small number of damaged cells. Cells treated with COS showed the significant decrease of damaged cells compare with control group.

7. Confirm of apoptotic cell death by TUNEL assay

Terminal Transferase dUTP Nick End Labeling (TUNEL) Assay is a method used to detect DNA degradation in apoptotic cells because one of the hallmarks of late stage apoptosis is the fragmentation of nuclear chromatin which results in a multitude of 3'-hydroxyl termini of DNA ends. This property can be used to identify apoptotic cells by labeling the DNA breaks with fluorescent-tagged deoxyuridine triphosphate nucleotides (F-dUTP). The enzyme terminal deoxynucleotidyl transferase (TdT) catalyzes a template-independent addition of deoxyribonucleoside triphosphates to the 3' hydroxyl ends of double- or single-stranded DNA generates DNA strands with exposed 3'-hydroxyl ends. To confirm the ability of COS to inhibit apoptosis, cells were treated with COS and the results are shown in Fig. 17. Control group, cells treated only A β , showed the strong detection of staining, whereas no staining was detected in untreated cell. Cells treated with COS appeared the reduction of TUNEL-positive detection.

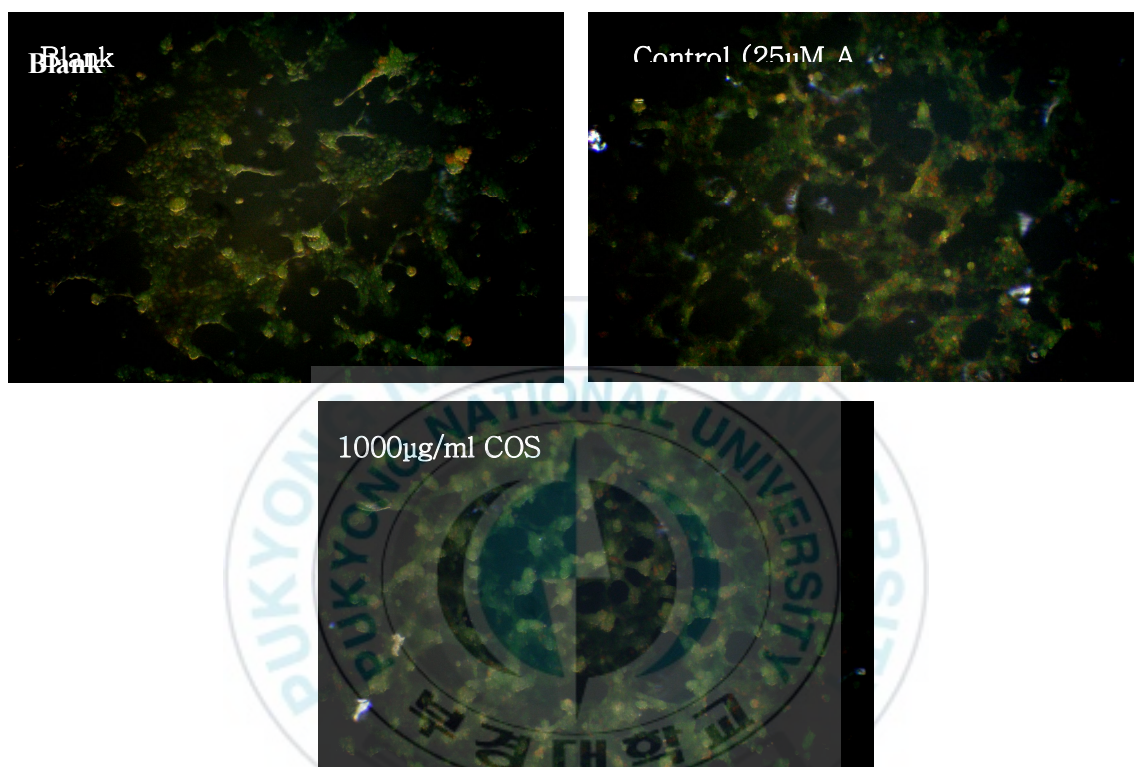


Figure 16. Morphological analysis of pc-12 treated with 1000 μg and $\text{A}\beta$ (25 μM) for 24 h.

Cells treated with COS were visualized with fluorescent microscope and compared with blank (non-treated cell) and control (only treated 25 μM $\text{A}\beta$).

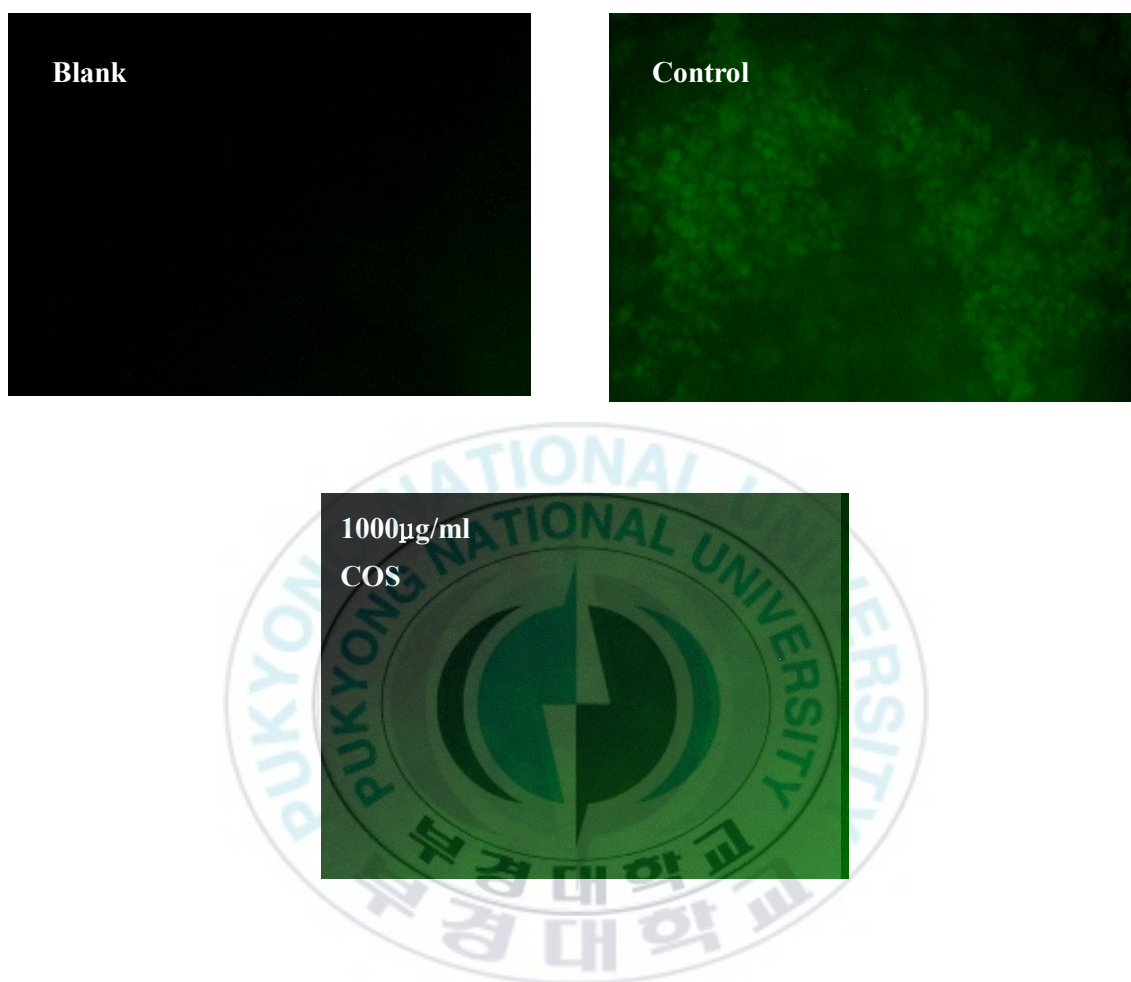


Figure 17. TUNEL stained cells after 24 h of treatment. Pc-12 cells were treated with 1000 μ l of COS and A β (25 μ M) after 24 h TUNEL assay was employed to identify apoptotic cells having free 3'-OH of cleaved DNA. TUNEL assay was performed using a kit according to manufacturer's instructions described in method. FITC-labelled cells were visualized with fluorescent microscope and compared with blank (non-treated cell) and control (only treated 25 μ M A β).

8. Determination of apoptosis by cell cycle

To study how COS affect the cell cycle progression, following treatment of COS at different concentration pc-12 cells were monitored for 24 h. Cell cycle analysis data obtained with PI staining revealed that cell cycle progression was delayed at S phase when cells were treated with A β ₂₅₋₃₅. After COS was added to the cell, the ratio of arrest of S phase was decreased in dose-dependant manner (Fig. 18). Significant number of apoptotic cells was observed after 24 h treatment of A β ₂₅₋₃₅. Few cells went through the apoptosis in non-treated cells. However, after treatment of COS to the cells, the number of apoptotic cells was decreased in dose-dependent manner (Fig. 19).



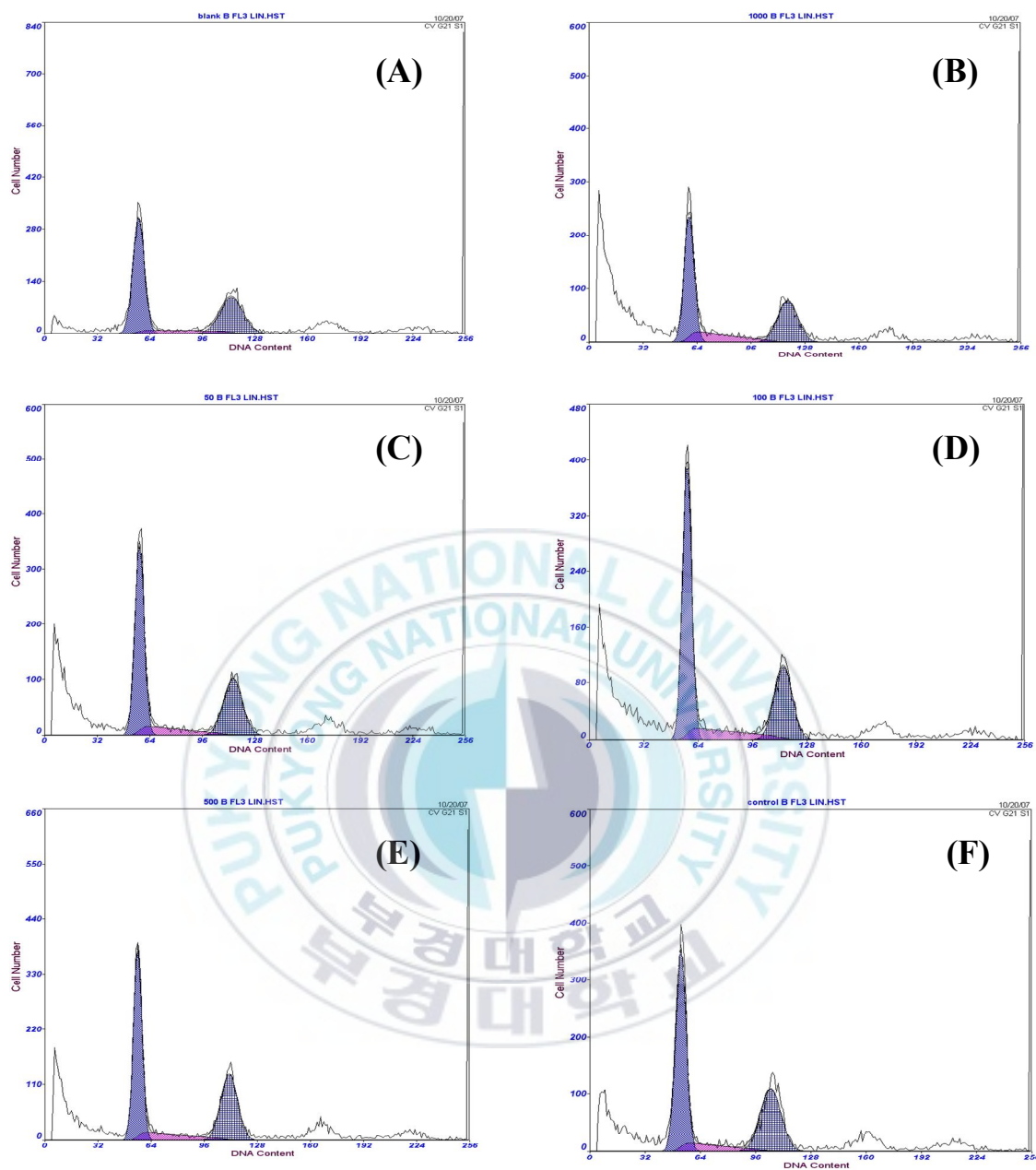


Figure 18. Cells cycle analysis of pc-12 cells in the presence of COS. Cells were treated with indicated concentrations of COS and A β (25 μ M) and harvested after 24 h. Propidium iodide staining was used to quantify cells undergoing apoptosis and to analyze the cell cycle using flow cytometer. A: Blank (non-treated cells), B: Control (only A β treated cells), C: 50 μ g/ml, D: 100 μ g/ml, E: 500 μ g/ml, F: 1000 μ g/ml.

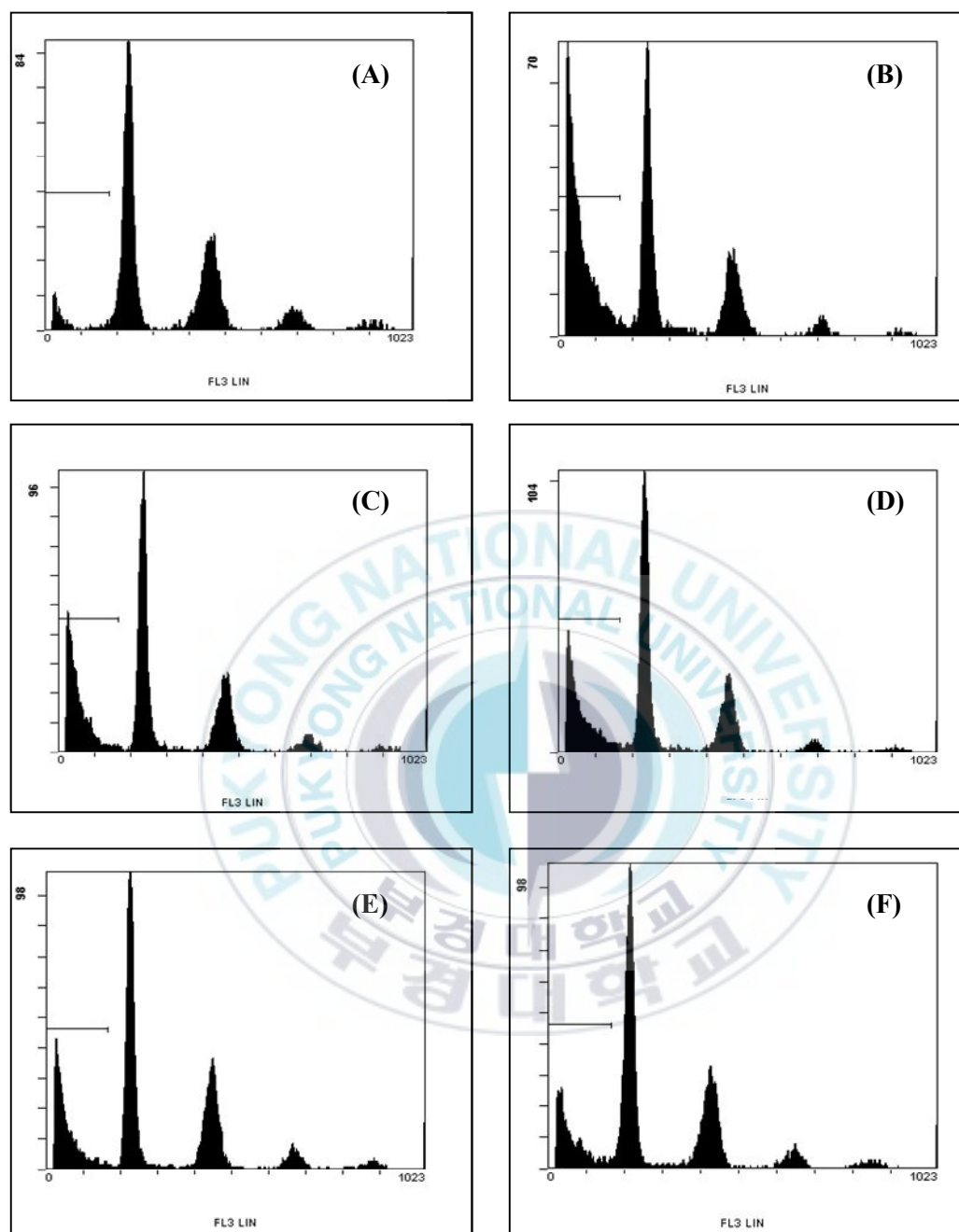


Figure 19. Quantification of apoptosis in pc-12 cells treated with COS after PI staining. Cells were treated with different concentrations of COS and A β (25 μ M) for 24 h. Propidium iodide staining was used to quantify cells undergoing apoptosis and to analyze the cell cycle. A: Blank (non-treated cells), B: Control (only A β treated cells), C: 50 μ g/ml, D: 100 μ g/ml, E: 500 μ g/ml, F: 1000 μ g/ml.

9. COS inhibit apoptosis via reduction of p53 expression level

Because p53 is important gene in the arrest of cell cycle, expression level of p53 was measured. To investigate the effect of COS in inhibition of apoptosis related with p53 in pc-12 cells induction of p53 was assessed at different gene expression levels. The level of p53 transcription was quantified using Real-time PCR performed with primer corresponding p53 gene. Data revealed that the gene expression level of COS treated groups was decreased compared with control groups. It means that COS can inhibit p53 transcription step, therefore, it is potent inhibitor of p53 gene expression in a dose-dependant manner (Fig. 20).

Because of the mechanism of p53 activation in respond to apoptosis inducing agents involves in mainly posttranslational modifications, including phosphorylation (Giaccia et al. 1998), western blot was carried out to investigate the reduction of total p53 and phosphor p53 using antibodies after treatment of COS and A β ₂₅₋₃₅ for 24 h. Protein expression of p53 was reduced in a dose-dependent manner. Moreover, phosphor p53 also appear similar result with total p53. Induction of these active forms of p53 was much lower than protein expression level of control treated with only A β ₂₅₋₃₅ without COS (Fig. 21).

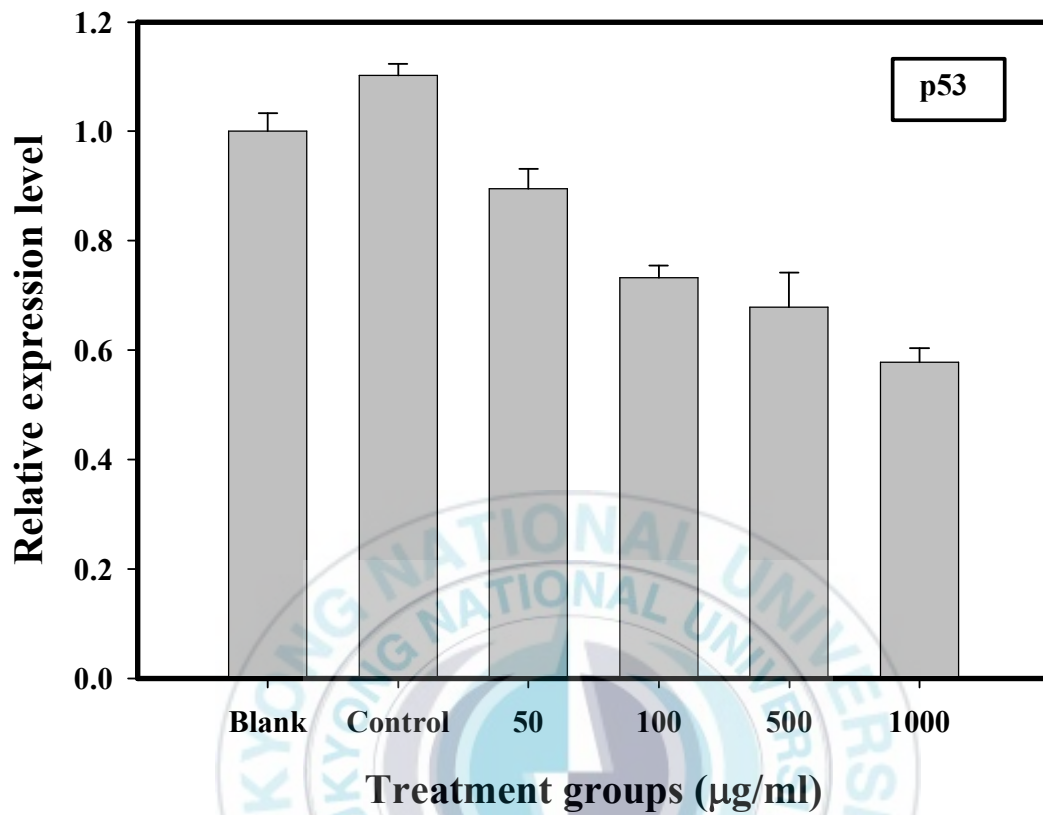


Figure 20. p53 mRNA expression in COS treated pc-12 cells. Different concentrations of COS treated pc-12 cells were incubated for 24 h and total RNA was extracted as described in method section. For real-time PCR, 1 µg of RNA was reverse-transcribed to generate first strand cDNA using AMV reverse transcriptase by reverse transcription (RT). RT-generated cDNA was used as a template to amplify p53 mRNA. Specific upstream and downstream primers were employed for the reaction.

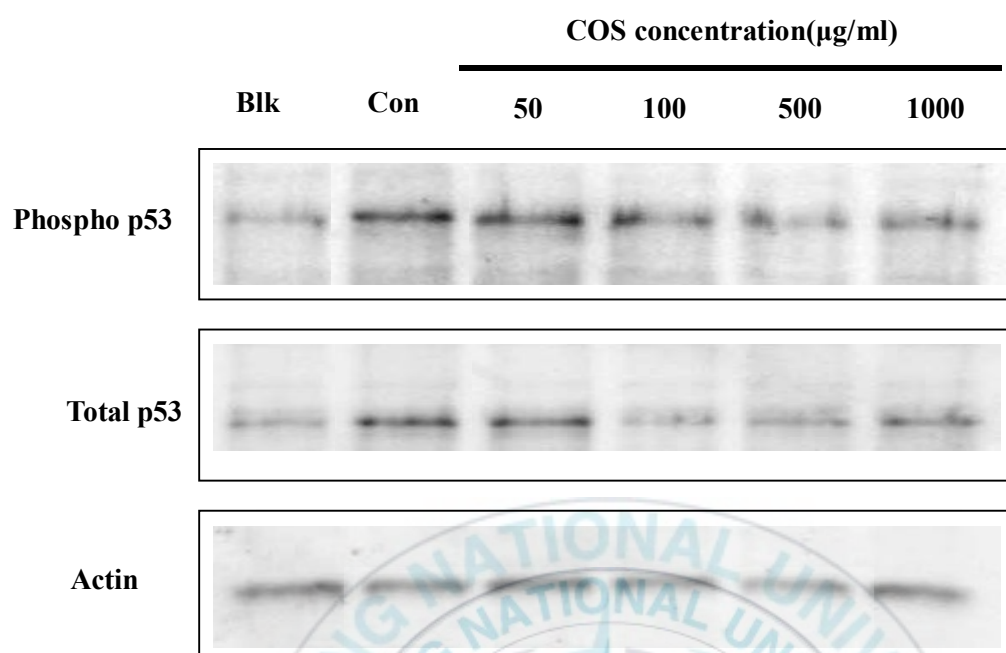


Figure 21. Western blot assay of p53 protein expression in pc-12 cells treated with COS. After treatment of COS and A β (25 μM) for 24 h, cell extracts were resolved by SDS-PAGE. Protein were transferred onto nitrocellulose membranes and incubated with antibodies. Western blot bands were developed with enhanced chemiluminescence reagents and visualized using LAS3000[®] Luminescent image analyzer. Actin was used for confirmation of equal amount of protein. Blk: non-treatment group; Con: only A β (25 μM) treatment group.

10. COS inhibit target genes in apoptosis pathway that affected by A β ₂₅₋₃₅

Since p53 inhibits cell growth through activation of cell cycle arrest and apoptosis, protein expression level of p21 and MDM2 that are critically involved in either cell growth arrest or apoptosis was assessed in the presence of COS. Western blot analysis carried out with anti MDM2 antibody exhibited that treatment of COS increased the protein level of MDM2 (Fig. 22). This increment is favorable for the transcriptional inactivation of p53 because MDM bind to the p53 and inhibits its ability to act as a transcription factor.

When the effect of COS on the induction of p21 was assessed, the protein expression level of p21 was decreased in dose-dependent manner. These data are in agreement with the reporter data that expression of p53 induces growth arrest via transcriptional activation of the cyclin-dependent kinase inhibitor p21.

Real-time PCR and western blot analysis was performed with corresponding Bcl-2 gene and anti-Bcl-2 antibody. The result clearly showed that COS activated Bcl-2 gene expression (Fig. 23) and protein expression level (Fig. 25). In contrast, Bax was down-regulated in a dose-dependent manner in both stages (Fig. 24 and 25). It means that COS can affect not only transcription stage but also translation stage. These result suggested that COS inhibited apoptosis partly by the alteration of the ratio of Bcl-2/Bax protein expression that directly affected the release of cytochrome c via alteration of mitochondria membrane permeability.

Further, COS reduced cytochrome c and Apaf-1 protein levels in pc-12 cells (Fig. 26). Also this result followed a similar pattern to reduction of Bax. These data are in agreement with the fact that during apoptosis, cytochrome c is released from mitochondria into the cytoplasm, by the Bax via alteration of membrane permeability. With this observation, in order to assess the effect of COS to reduce Apaf-1, protein expression levels of Apaf-1 in the presence of COS were tested following the same treatment duration. A significant reduction of Apaf-1 protein

compare to that of control group was observed following treatment of COS to cells. In control group, a strong expression level was observed whereas COS decreased the expression of Apaf-1 protein level in a dose-dependant manner.



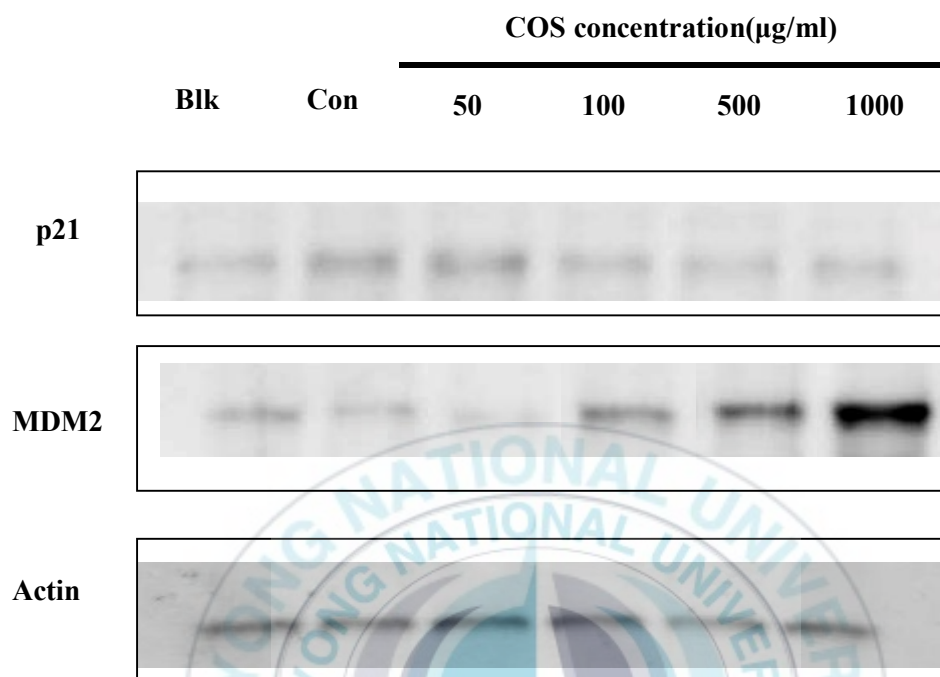


Figure 22. Western blot assay of MDM2 and p21 protein expression in pc-12 cells treated with COS. After treatment of COS and A β (25 μM) for 24 h, cell extracts were resolved by SDS-PAGE. Protein were transferred onto nitrocellulose membranes and incubated with antibodies. Western blot bands were developed with enhanced chemiluminescence reagents and visualized using LAS3000[®] Luminescent image analyzer. Actin was used for confirmation of equal amount of protein. Blk: non-treatment group; Con: only A β (25 μM) treatment group.

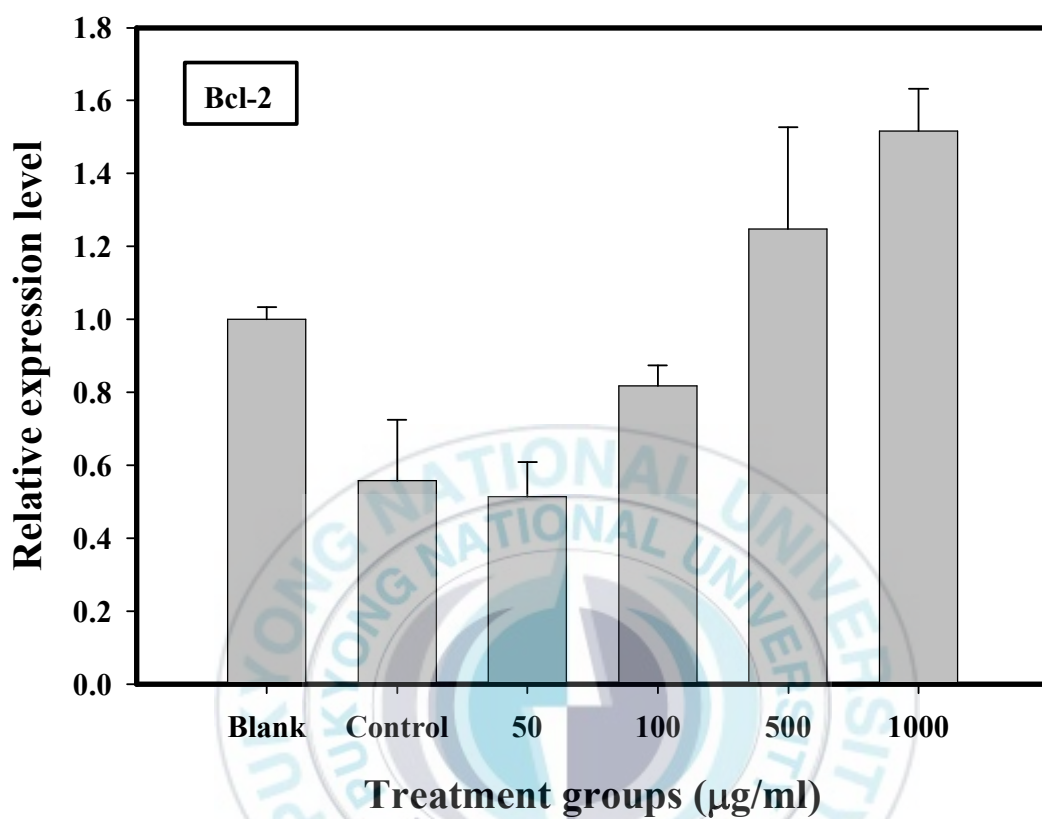


Figure 23. Bcl-2 mRNA expression level treated pc-12 cells. Different concentrations of COS treated pc-12 cells were incubated for 24 h and total RNA was extracted as described in method section. For real-time PCR, 1 µg of RNA was reverse-transcribed to generate first strand cDNA using AMV reverse transcriptase by reverse transcription (RT). RT-generated cDNA was used as a template to amplify Bcl-2 mRNA. Specific upstream and downstream primers were employed for the reaction.

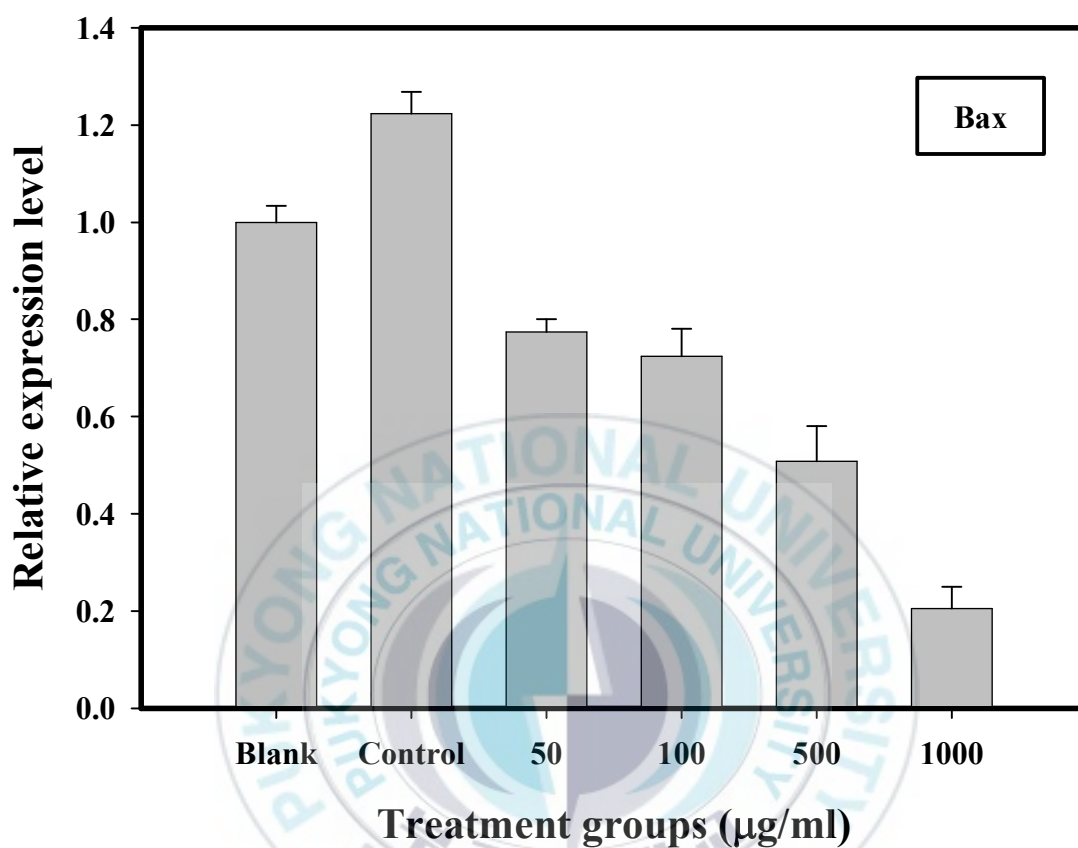


Figure 24. Bax mRNA expression level in COS treated pc-12 cells. Different concentrations of COS treated pc-12 cells were incubated for 24 h and total RNA was extracted as described in method section. For real-time PCR, 1 μg of RNA was reverse-transcribed to generate first strand cDNA using AMV reverse transcriptase by reverse transcription (RT). RT-generated cDNA was used as a template to amplify Bax mRNA. Specific upstream and downstream primers were employed for the reaction.

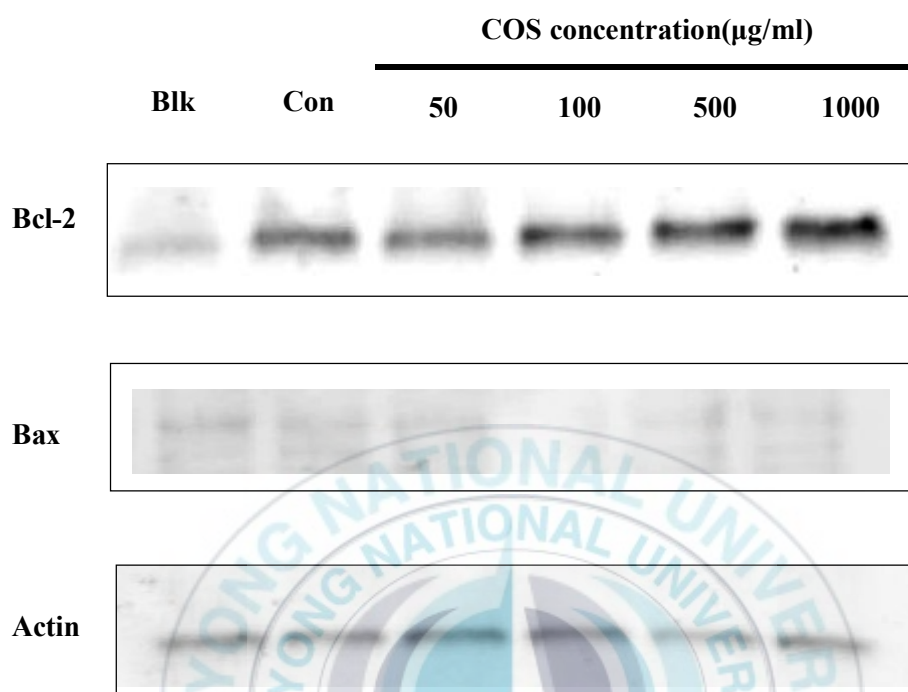


Figure 25. Western blot assay of Bax and Bcl-2 protein expression in pc-12 cells treated with COS. After treatment of COS and A β (25 μM) for 24 h, cell extracts were resolved by SDS-PAGE. Protein were transferred onto nitrocellulose membranes and incubated with antibodies. Western blot bands were developed with enhanced chemiluminescence reagents and visualized using LAS3000[®] Luminescent image analyzer. Actin was used for confirmation of equal amount of protein. Blk: non-treatment group; Con: only A β (25 μM) treatment group.

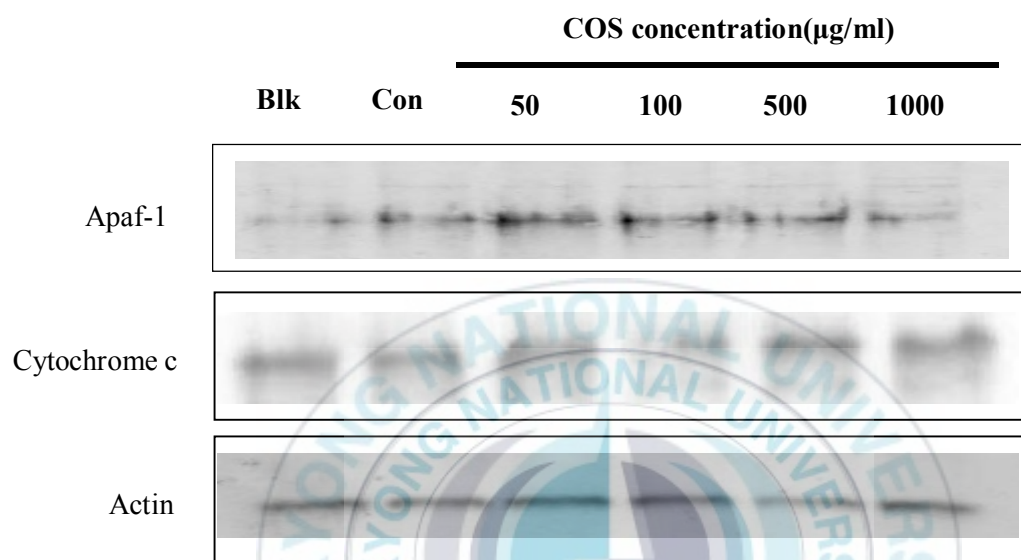


Figure 26. Western blot assay of Apaf-1 and cytochrome C protein expression in pc-12 cells treated with COS. After treatment of COS and A β (25 μM) for 24 h, cell extracts were resolved by SDS-PAGE. Protein were transferred onto nitrocellulose membranes and incubated with antibodies. Western blot bands were developed with enhanced chemiluminescence reagents and visualized using LAS3000[®] Luminescent image analyzer. Actin was used for confirmation of equal amount of protein. Blk: non-treatment group; Con: only A β (25 μM) treatment group.

Besides, the reduction of caspase-9 expression was observed in the presence of COS (Fig.27, 29). This result was an expected result because processed caspase-9 remains associated with the apoptosome as a holo-enzyme to maintain its catalytic activity (Rodriguez et al. 1999) and apoptosome serves as an allosteric regulator for the enzymatic activity of caspase-9. Reduction in the apoptosome in the presence of COS confirmed its anti-apoptotic potential since Apaf-1/caspase-9 pathway mediates a variety of apoptotic stimuli. In line with reduction of caspase-9 a simultaneous reduction of caspase-3 level was observed in Real-time PCR and western blot data (Fig.28, 29). Apoptosis is executed by a cascade of caspase activation. (Thornberry et al.1998). The activation of an effector caspase, such as caspase-3, is performed by an initiator caspase, such as caspase-9, through proteolytic cleavage at specific Asp residues. Therefore, the inactivation of initiator caspase, caspase-9 in the presence of COS can inactivate the effector caspases and subsequently inhibit the cleavage of numerous cellular targets, leading to cell death. In addition, in order to confirm the effect of COS on the function and inhibition of caspase members functioning in extrinsic pathway of apoptosis, protein level of caspase-8 was assessed following treatment of COS in a dose-dependent manner (Fig. 29).

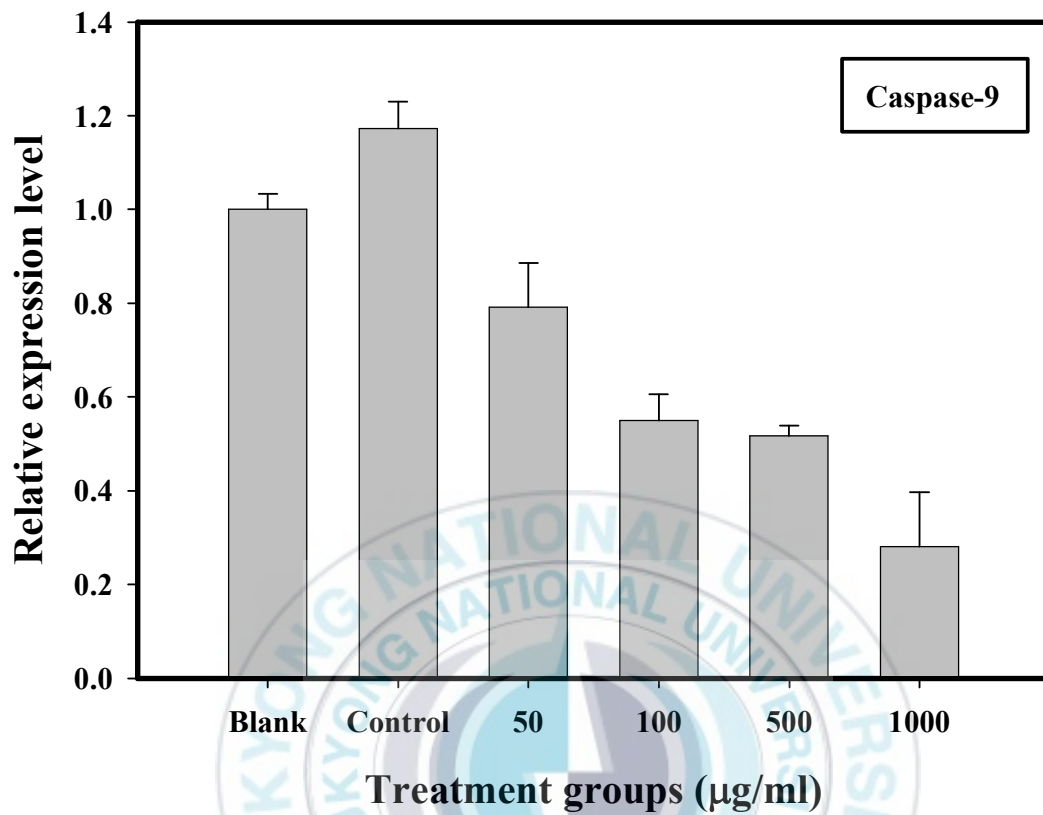


Figure 27. Caspase-9 mRNA expression level in COS treated pc-12 cells. Different concentrations of COS treated pc-12 cells were incubated for 24 h and total RNA was extracted as described in method section. For real-time PCR, 1 µg of RNA was reverse-transcribed to generate first strand cDNA using AMV reverse transcriptase by reverse transcription (RT). RT-generated cDNA was used as a template to amplify Caspase-9 mRNA. Specific upstream and downstream primers were employed for the reaction.

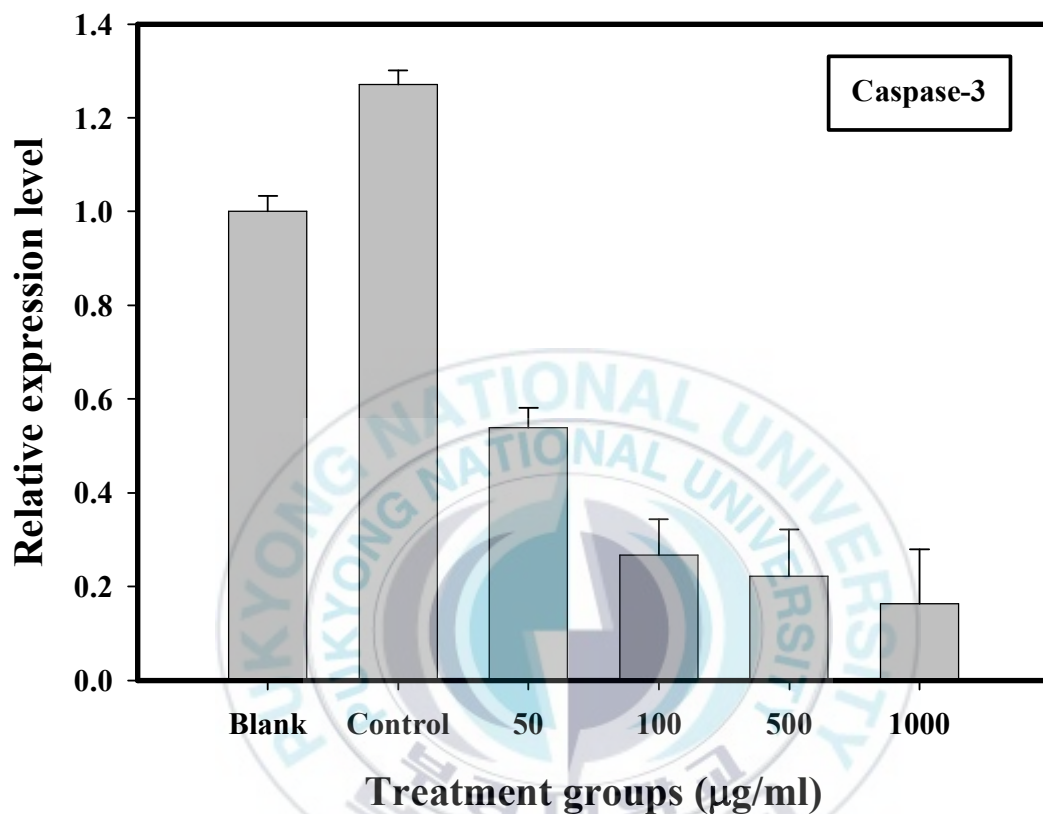


Figure 28. Caspase-3 mRNA expression in COS treated pc-12 cells. Different concentrations of COS treated pc-12 cells were incubated for 24 h and total RNA was extracted as described in method section. For real-time PCR, 1 µg of RNA was reverse-transcribed to generate first strand cDNA using AMV reverse transcriptase by reverse transcription (RT). RT-generated cDNA was used as a template to amplify Caspase-3 mRNA. Specific upstream and downstream primers were employed for the reaction.

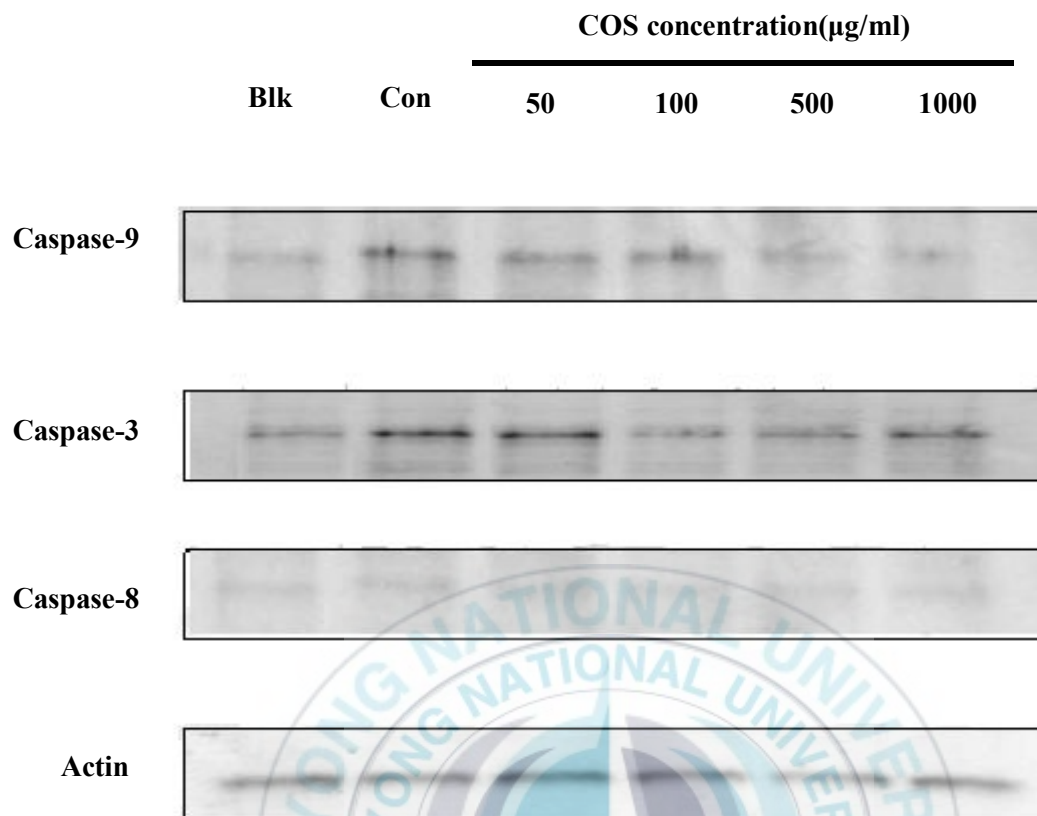


Figure 29. Western blot assay of caspase-9, caspase-3 and caspase-8 protein expression in pc-12 cells treated with COS. After treatment of COS and A β (25 μM) for 24 h, cell extracts were resolved by SDS-PAGE. Protein were transferred onto nitrocellulose membranes and incubated with antibodies. Western blot bands were developed with enhanced chemiluminescence reagents and visualized using LAS3000[®] Luminescent image analyzer. Actin was used for confirmation of equal amount of protein. Blk: non-treatment group; Con: only A β (25 μM) treatment group.

Summary

A β is a cause of neuronal apoptosis and acetylcholinesterase (AChE) plays a significant role in modulating the cytotoxicity of A β . Therefore, it was necessary to investigate inhibitory effect of COS in AChE activity. The result revealed that COS could reduce AChE activity so it is helpful to treat Alzheimer's disease.

In this research, COS was used as an inhibitor of neuronal apoptosis which is a cause of Alzheimer's disease. Among various molecular of COS, 3~5 kDa COS was selected for this study, 3~5 kDa COS is the most effective to inhibit the formation of ROS so it can inhibit cell death induced by A β_{25-35} in the pc-12 cells. Cell morphological assay and TUNEL assay confirmed that A β_{25-35} killed pc-12 cells by inducing apoptosis but COS can inhibit apoptosis. Further, cell cycle analysis of pc-12 cells revealed that cell cycle progression was delayed at S phase in the presence of A β_{25-35} but COS decreased arrest of S phase in dose-dependent manner. Because p53 is related to the cell cycle arrest, it was necessary to evaluate p53 expression level. In real-time PCR and western blot assay, gene and protein expression levels of p53 were gradually decreased when the cells were treated with COS. It means that COS can inhibit p53 related apoptosis pathway. Concurrently, the reduction in protein expression levels of cytochrom C, Apaf-1 and caspase-9 confirmed that COS inhibited a mitochondria pathway of apoptosis in pc-12 cells. This result indicated that COS obstructed the alteration of mitochondrial membrane permeability that determined from reduction of Bax and increment in anti-apoptotic protein Bcl-2. The reduction of Apaf-1 level in the presence of COS found to be affecting to control cascade of signaling events subsequently (Fig. 30).

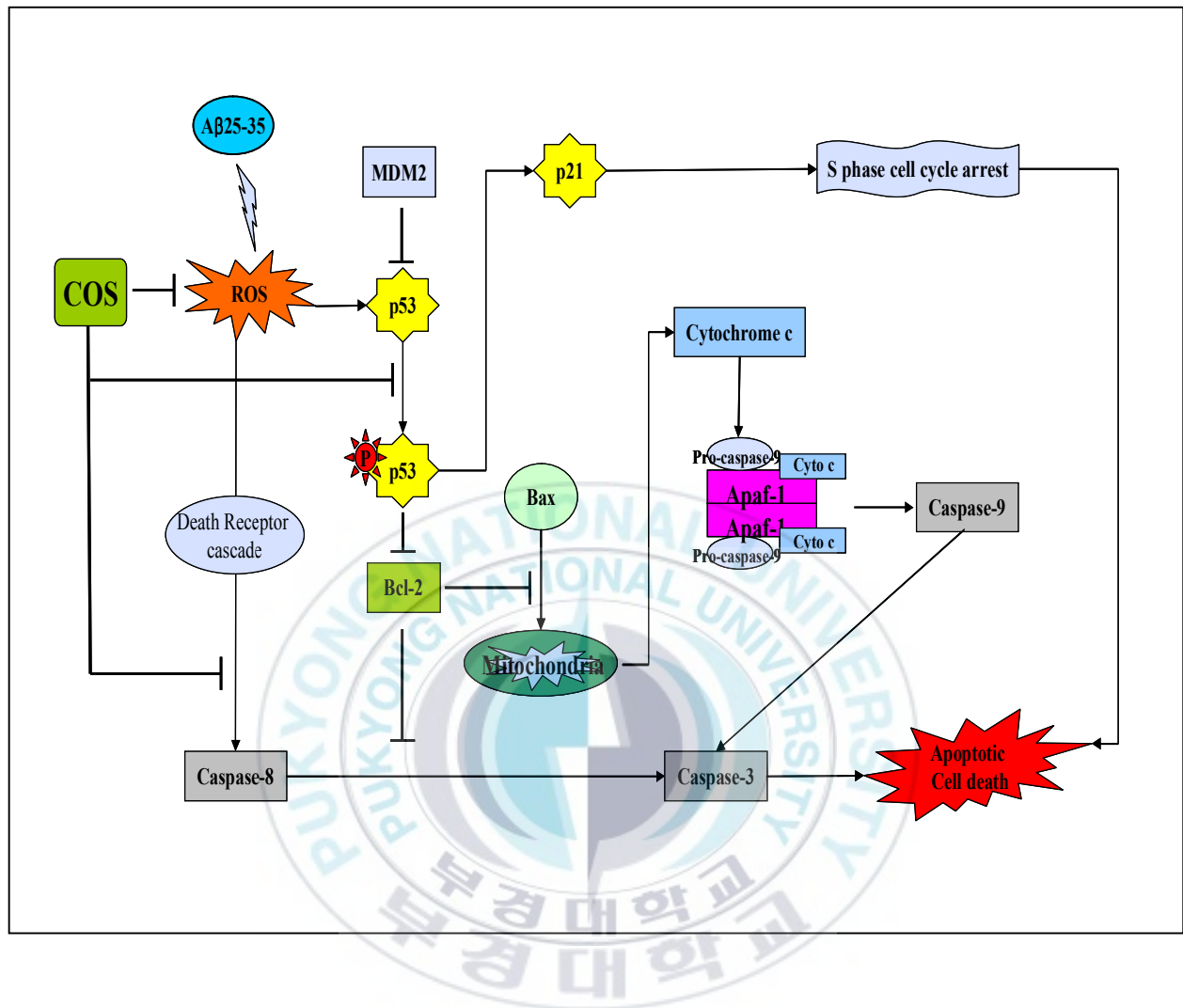


Figure 30. The proposed signaling cascade in pc-12 cells affected by COS. $A\beta_{25-35}$ induced apoptosis via p53 signaling cascade and mitochondria pathway. When COS was treated into the pc-12 cell apoptotic signaling of this cascade was inhibited.

References

1. Allan, G.R. and Hadwiger, L.A. The fungicidal effect of chitosan on fungi of varying cell wall composition. *Exp. Mycol.* (1979). 3:285-287.
2. Alvarez A, Alarcon R, Opazo C, Campos EO, Munoz FJ, Calderon FH, et al. Stable complexes involving acetylcholinesterase and amyloid-beta peptide change the biochemical properties of the enzyme and increase the neurotoxicity of Alzheimer's fibrils. *J Neurosci* (1998). 18: 3213-23.
3. Ames B, Shingenaga M, Park EM. Oxidation damage and repair: chemical, biological and medical aspects. Elmsford, United Kingdom: Pergamon Press (1991).
4. Andrea C. LeBlanc. The Role of Apoptosis Pathway in Alzheimer's Disease Neurodegeneration and Cell Death. *Current Alzheimer Research* (2005). 2:389-402.
5. Beal MF, Howell N, Bodis-Wollner IB, eds. Mitochondria and free radicals in neurodegenerative diseases. New York: Wiley-Liss (1997)
6. Butterfield, D. A., Hensley, K., Harris, M., Mattson, M. P., and Carney, J. M. β -Amyloid peptide free radical fragments initiate synaptosomal lipoperoxidation in a sequence-specific fashion: Implications to Alzheimer's disease, *Biochem. Biophys. Res. Commun* (1994). 200:710–715.
7. Calderon FH, Von Bernhardt R, De Ferrari G, Luza S, Aldunate R, Inestrosa NC. Toxic effects of acetylcholinesterase on neuronal and glial-like cells in vitro. *Mol Psychiatry* (1998). 3: 247-55
8. Colurso GJ, Nilson JE and Vervoort LG. Quantitative assessment of DNA fragmentation and beta-amyloid deposition in insular cortex and midfrontal gyrus from

- patients with Alzheimer's disease. *Life Sci* (2003). 73:1795-1803.
9. Cooper AJL. Glutathione in the brain: disorders of glutathione metabolism. In: Rosenberg RN, Prusiner SB, DiMauro S, Barchi RL, Klunk LM, eds. *The molecular and genetic basis of neurological disease*. Boston: Butterworth-Heinemann (1997). 1242–5.
 10. Corain, B., Iqbal, K., Nicolini, M., Winblad, B., Wisniewski, H., and Zatta, P. (Eds.). *Alzheimer's Disease: Advances in Clinical and Basic Research*, Wiley, New York. (1993).
 11. D.J. Selkoe, Translating cell biology into therapeutic advances in Alzheimer's disease. *Nature* 399 (1999) A23–A31.
 12. Ding, H.F. and Fisher, D.E. Mechanisms of p53-mediated apoptosis. *Crit. Rev. Oncog.* (1998). 9:83-98.
 13. Frances H. Calderon, Andrea Bonnefont, Francisco J. Munoz, Virginia Fernandez, Luis A. Videla, and Nibaldo C. Inestrosa. PC12 and Neuro 2a cells have different susceptibility to acetylcholinesterase-amyloid complex, amyloid 25-35 fragment, glutamate, and hydrogen peroxide. *Journal of Neuroscience Research* (1999). 56:620-631.
 14. Frank M. LaFerla, Kim N. Green and Salvatore Oddo (2007). Intracellular amyloid- β in Alzheimer's disease. *Nature Review, Neuroscience* 8: 499-509.
 15. Friedlander RM. Apoptosis and caspases in neurodegenerative diseases. *N Engl J Med.* (2003). 348:1365-1375.
 16. Giaccia, A. J. and Kastan, M. B. The complexity of p53 modulation: emerging patterns from divergent signals. *Gene Dev.* (1998). 12:2973-2983.
 17. Giorgio Silvestelli, Alessia Lanari, Lucilla Parnetti, Daniele Tomassoni, Francesco

- Amenta. Treatment of Alzheimer's disease: From pharmacology to a better understanding of disease pathophysiology. *Mechanism of Aging and Development* (2006). 127:148-157.
18. Hadwiger, L. A. and Beckman, J.M, Chitosan as a component of pea-Fusarium solani interactions. *Plant Physiol.* (1980). 66:205-211.
19. Halliwell B. Free radicals, antioxidants, and human disease: curiosity, cause, or consequence. *Lancet* (1994). 344:721-724.
20. Hazel JR, Williams EE. The role of alterations in membrane lipid composition in enabling physiological adaptation of organisms to their physical environment. *Prog Lipid Res* (1990). 29:167-227.
21. Hee-Guk Byun, Yong-Tae Kim, Pyo-Jam Park, Xinli Lin, and Se-Kwon Kim. Chitooligosaccharides as a novel β -secretase inhibitor. *Carbohydrate Polymers* (2005). 61:198-202.
22. Hensey K, Hall N, Subramaniam R, et al. Brain regional correspondence between Alzheimer's disease histopathology and biomarkers of protein oxidation. *J Neurochem* (1995). 65:2146-56.
23. Hirano, S and Nagao, N. Effects of chitosan, pectic acid, lysozyme, and chitinase on the growth of several phytopathogens. *Agric. Bio. Chem.* (1989). 53:3065-3066
- hydrogen-peroxide- and peroxynitrite-induced apoptosis of PC12 cells by blocking down-regulation of Bcl-XL and activation of JNK. *Journal of Nutritional Biochemistry* (2007).
24. Hyo Jin Kima, Ki Won Leeb, Mi-Sung Kim, Hyong Joo Lee. Piceatannol attenuates
25. I. Blasko, M. Wagner, N. Whitaker, B. Grubeck-Loebenstien, P. Jansen-Durra. The amyloid- β peptide A β (25-35) induces apoptosis independent of p53. *FEBS Letters* (2000). 470:221-225

26. J.A. Hardy, G.A. Higgins, Alzheimer's disease: the amyloid cascade hypothesis. *Science* (1992). 256:184–185.
27. J.A. Johnston, W.W. Liu, D.T.R. Coulson, S. Todd, S. Murphy, S. Brennan, C.J. Foy, D. Craig, G.B. Irvine, A.P. Passmore. Platelet β -secretase activity is increased in Alzheimer's disease. *Neurobiology of Aging* (2006).
28. Jang J-H, Surh Y-J. Potentiation of cellular antioxidant capacity by Bcl-2: implications for its antiapoptotic function. *Biochem Pharmacol* (2003). 66:1371–9.
29. Jung-Hee Jang and Young-Joon Surh. Bcl-2 protects against A β 25–35-induced oxidative PC12 cell death by potentiation of antioxidant capacity. *Biochemical and Biophysical Research Communications* (2004). 320:880–886.
30. Kaj Blennow, Mony J de Leon, Henrik Zetterberg. Alzheimer disease. *Lancet* (2006); 368: 387–403.
31. Katzman, R., and Saitoh, T. Advances in Alzheimer's disease, *FASEB J* (1991). 4:278–286.
32. Kazuhiro Takuma, Shirley ShiDu Yan, David M. Stern, and Kiyofumi Yamada Mitochondrial Dysfunction, Endoplasmic Reticulum Stress, and Apoptosis in Alzheimer's Disease. *J Pharmacol Sci* (2005). 97: 312-316
33. LI-JUN ZHOU and XING-ZU ZHU. Reactive Oxygen Species-Induced Apoptosis in PC12 Cells and Protective Effect of Bilobalide. *The Journal of Pharmacology and Experimental Therapeutics* (2000). 293:982-988.
34. LI-JUN, ZHOU and XING-ZU ZHU. Reactive Oxygen Species-Induced Apoptosis in PC12 Cells and Protective Effect of Biobalide. *The Journal of Phamacology* (2000). 293:982-988.
35. Li-Zhen Wang, Wan-Chun Sun, Xing-Zu Zhu. Ethyl pyruvate protects PC12 cells from

- dopamine-induced apoptosis. *European Journal of Pharmacology* (2005). 508 57-68.
36. Mark A. Smith, Catherine A. Rotkamp, Akihiko Nunomura, Arun K. raina, George Perry. Oxidative stress in Alzheimer's disease. *Biochimica et Biophysica Acta* (2000).502:139-144
37. Mark P. Mattson. Apoptosis in neurodegenerative disorders. *Nature reviews molecular biology* (2000). 1:120-129.
38. Mark RJ, Lovell MA, Markesbery WR, Uchida K, Mattson MP. A role for 4-hydroxynonenal, an aldehydic product of lipid peroxidation, in disruption of ion homeostasis and neuronal death induced by amyloid β -peptide. *J Neurochem* (1997). 68:255–64
39. Mark RJ, Lovell MA, Markesbery WR, Uchida K, Mattson MP. A role for 4-hydroxynonenal, an aldehydic product of lipid peroxidation, in disruption of ion homeostasis and neuronal death induced by amyloid b-peptide. *J Neurochem* (1997). 68:255–64.
40. Markesbery WR, Lovell MA. Four-hydroxynonenal, a product of lipid peroxidation, is increased in the brain in Alzheimer's disease. *Neurobiol Aging* (1998). 19:33–6
41. Markesbery, W. R. Oxidative stress hypothesis in Alzheimer disease, *Free Rad. Biol. Med* (1997). 23:134–147.
42. Markesbery, W. R., and Carney, J. M. Oxidative alterations in Alzheimer's disease, *Brain Pathol.* (1999). 9:133–146.
43. Masters, C. L. et al. Amyloid plaque core protein in Alzheimer disease and Down syndrome. *Proc. Natl Acad. Sci. USA* (1985) 82: 4245–4249.
44. Matura T, Kai M, Fujii Y, Ito H and Yamada K. Hydrogen peroxide-induced apoptosis in HL-60 cells requires caspase-3 activation. *Free Radic Res* (1999). 30:73-83.

45. Mecocci P, MacGarvey U, Beal MF. Oxidative damage to mitochondrial DNA is increased in Alzheimer's disease. *Ann Neurol* (1994). 36:747–51.
46. Niranjana Rajapakse, Moon-Moo Kim, Eresha Mendis and Se-Kwon Kim. Inhibition of free radical-mediated oxidation of cellular biomolecules by carboxylated chitooligosaccharides. *Bioorganic & Medicinal Chemistry* (2007). 15: 997-1003.
47. Okuda, H. Kato, H. and Tsujita, T. Antihypertensive and antihyperlipemic actions of chitosan. *J. Chitin chitosan* (1997). 2:49-59.
48. Oltvai Z, Millman C, Korsmeyer SJ. Bcl-2 heterodimerizes in vivo with a conserved homolog, Bax, that accelerates programmed cell death. *Cell* (1993). 74:609–619.
49. Overmyer M, Kraszpulski M, Helisalmi S, Soininen H and Alafuzoff I. DNA fragmentation, gliosis and histological hallmarks of Alzheimer's disease. *Acta Neuropathol (Berl)* (2000). 100:681-687.
50. Pawel Kermer, Jan Liman, Jochen H. Weishaupt and Mathias Bahr. Neuronal Apoptosis in Neurodegenerative Diseases: From Basic Research to Clinical Application. *Neurodegenerative Dis* (2004). 1:9-19.
51. Roberta Borghi, Stefania Patriarca, Nicola Traverso, Alessandra Piccini, Daniela Storace, Anna Garuti, Gabriella Cirmena, Patrizio Odetti, Massimo Tabaton. The increased activity of BACE1 correlates with oxidative stress in Alzheimer's disease. *Neurobiology of Aging* (2006).
52. Sanjiv Shah and Gang Yu. sorLA: Sorting Out APP. *Molecular interventions* (2006). 6:74-76.
53. Selkoe DJ. Alzheimer's disease: Genes, proteins, and therap. *Physiol Rev* (2001). 81: 741–66.
54. Selkoe, D. J. The molecular pathology of Alzheimer's disease, *Neuron* (1991). 6:487–

498.

55. Shinobu Kitazume, Takaomi C. Saido and Yasuhiro Hashimoto Alzheimer's β -secretase cleaves a glycosyltransferase as a physiological substrate Glycoconjugate Journal (2004). 20:59–62
56. Smith MA, Rudnicka-Nawrot M, Richey PL, et al. Carbonyl-related posttranslational modification of neurofilament protein in the neurofibrillary pathology of Alzheimer's disease. J Neurochem (1995). 64:2660–6.
57. Sridhar Varadarajan, Servet Yatin, Marina Aksenova, and D. Allan Butterfield. Review: Alzheimer's Amyloid β -Peptide-Associated Free Radical Oxidative Stress and Neurotoxicity Journal of Structural Biology (2000). 130:184–208.
58. Uchida, Y., Izume, M and Ohtakara, A. Preparation of chitosan oligomers with purified chitosanase and its application. In Chitin and Chitosan. Skjak-Brak, G. Anthonsen, T. and Sandford, P. (eds). UK, Elsevier Applied Science (1989). 373-382.
59. Walker-Simmons, M., Hadwiger, L. and Ryanee, C.A. Chitosans and pectic polysaccharides both induce the accumulation of the antifungal phytoalexin pisatin in pea pods and antinutrient proteinase inhibitors in tomato leaves. Biochem. Biophys. Res. Commun. (1983). 110:194-199.
60. Walsh, D.M. and Selkoe, D.J. Deciphering the molecular basis of memory failure in Alzheimer's Disease. Neuron (2004). 44:181–193
61. Yan-Ping Li, Anne F.Bushnell, Chi-Ming Lee, Lynn S.Perlmutter, Stephen K.-F.Wong. β -Amyloid induces apoptosis in human-derived neurotypic SH-SY5Y cells. Brain Research (1996). 738:196-204.
62. Yoshihisa Kitamura, Takashi Taniguchi and Shun Shimohama. Apoptotic Cell Death in Neurons and Glial Cells: Implications for Alzheimer's Disease. japanese journal of

- pharmacology (1999). 79:1-5
63. Yves Christen. Oxidativd stress and Alzheimer disease. The American Journal of Clinical Nurition (2000). 71(suppl):621S-9S.
64. ZHANG Hai-Yan, Stephen BRIMIJOIN, TANG Xi-Can. Apoptosis induced by β -amyloid25-35 in acetylcholinesterase-overexpressing neuroblastoma cells. Acta Pharmacol Sin (2003). 24 (9): 853-858



Acknowledgment

해양 생화학 실험실에 들어 온지도 어느덧 2년이라는 시간이 훌쩍 넘어 이렇게 석사 학위를 받게 되었습니다. 이 논문이 완성되기까지 많은 도움과 관심을 주신 분들께 감사의 말씀을 전하고자 합니다.

먼저 지난 2년 동안 부족한 저에게 기회를 주시고 본 논문이 완성되기까지 언제나 세심한 배려로 돌보아주신 김세권 지도 교수님께 감사 드립니다. 그리고 부족한 논문을 따뜻한 격려와 충고로 심사하여 주신 심현관 교수님, 윤소원 교수님께 진심으로 감사 드립니다.

여러 가지로 부족한 이 논문이 완성되기까지 아낌없는 도움과 조언과 가르침을 주신 동의대 김문무 교수님, 정원교 박사님께도 감사의 말씀을 전합니다.

그리고 그 동안 함께 생활하면서 이 논문이 완성 되기 까지 저에게 많은 도움을 주신 강릉대 변희국 교수님, 전남대 제재영 교수님, Nghiep 선배님, 이상훈 선배님, 김희주 선배님, 엄태길 선배님, 천충길 선배님, 조영숙 선배님께 감사 드립니다. 그 밖의 실험실에서 함께 생활한 Van님, Murat님, To님을 비롯하여 김정애 후배님, Fatih 후배님, 류보미 후배님, 그리고 강경화 선생님, Dr. Khan, Dr. Dominic, Maria 님께도 감사의 인사를 드리고자 합니다.

마지막으로 오늘의 제가 있기까지 사랑과 믿음으로 그 누구보다 큰 힘이 되어준 사랑하는 부모님, 그리고 가족들에게 감사의 인사를 드리며 이 작은 결실의 기쁨을 나누고 싶습니다.

2008년 1월 실험실에서

박진숙 드림